Multiband structure and critical behavior of matrix models

Krešimir Demeterfi,* Nivedita Deo,† Sanjay Jain,‡ and Chung-I Tan
Department of Physics, Brown University, Providence, Rhode Island 02912
(Received 17 August 1990)

We discuss, perturbatively and nonperturbatively, the multiband phase structure that arises in Hermitian one-matrix models with potentials having several local minima. The tree-level phase diagram for the ϕ^6 potential including critical exponents at the phase boundaries is presented. The multiband structure is then studied from the viewpoint of the orthogonal polynomial recursion coefficients R_n, using the operator formalism to relate them to the large-N limit of the generating function $F(z)\equiv(1/N)\langle \mathrm{tr}1/(z-\Phi)\rangle$. We show how a periodicity structure in the sequence of the R_n coefficients naturally leads to multiband structure, and in particular, provide an explicit example of a three-band phase. Numerical evidence for the periodicity structure among the recursion coefficients is given. We then present examples where we identify the double-scaling limit from a multiband phase. In particular, a $(k=2)$-type multicritical nonperturbative solution from the two-band phase in the ϕ^8 potential, and a $(k=1)$-type nonperturbative solution from the three-band phase in the ϕ^6 potential is found. Both solutions are described by differential equations related to the modified Korteweg–de Vries hierarchy. Finally, we comment on the other phases that coexist with the $k=2$ pure gravity solution.

I. INTRODUCTION AND SUMMARY

Matrix models have proved to be a powerful tool for analyzing sums over random surfaces.[1,2] Their original development from the large-N expansion was motivated by the desire to understand the nonperturbative structure of QCD,[3–6] and recently they have been used to propose a nonperturbative definition[7–10] of certain toy models of noncritical strings.[11–13]

Nonperturbative solutions are obtained at special subspaces of the space of couplings of the matrix model where its free energy becomes singular and can be considered as defining a sum over random surfaces. It is a characteristic property of sums over random surfaces that when the susceptibility is singular, the singularity is systematically higher for every successive genus, the critical exponent γ_{str} growing linearly with genus.[12,14] This property allows the enhancement of higher-genus contributions close to the singularity by "double scaling" and obtaining a solution directly for their sum, which is then identified as a solution of a string model.

Since the matrix models provide the only nonperturbative definition of two-dimensional (2D) gravity and string theory via this identification, it is important to ask, within the context of the matrix models themselves, whether the subspace where such solutions have been obtained admits other solutions corresponding to other phases, particularly nonperturbative solutions, and if so to find their nature, discuss tunneling, etc. The question to be asked is, when is the matrix model in the first place well defined on this subspace? If the proposal of using these models to *define* the nonperturbative string theory is valid, the answer to this question constitutes information regarding the phase structure of string theory itself, which cannot be obtained within its usual formulation as a genus expansion. This was one motivation for this work. Another motivation is that, in general, at every critical line where double scaling is possible, the matrix model defines some continuum random surface theory. Thus the study of the various types of critical behavior exhibited by the matrix model is also of interest in its own right.

In this paper we address these issues for the simplest case—the Hermitian one-matrix model. This contains within its space of couplings a subspace where the solution obtained in Ref. 7 is characterized by the critical exponent $\gamma_{\mathrm{str}}\equiv -1/k=-\frac{1}{2}$ and is identified as being the solution of pure 2D gravity. Two questions that are relevant to the issues raised above and that we address in this paper are, first, what is the phase structure of a well-defined matrix model that exhibits a $k=2$ solution, including critical exponents at the phase boundaries, and, second, how can one obtain nonperturbative solutions that correspond to the other phases. We give the complete tree-level phase structure of the Hermitian one-matrix model U_6 (we refer to a model by its potential U_n, a polynomial of degree n), exhibit nonperturbative solutions for U_6 and U_8 corresponding to "multiband phases," and discuss some aspects of the kind of phase that can coexist with the pure gravity solution.

The $k=2$ solution also exists in the model U_3 and the "inverted Mexican-hat" model U_4, both unbounded from below. Thus U_6 is the simplest well-defined model containing a $k=2$ solution. Certain aspects of the tree-level phase structure of this model have recently also been studied by others;[15–17] results from these references overlap with part of Sec. II of the present paper. Other work on related questions includes discussion of the $k=3$ solution[18] occuring in U_6 and the impossibility of flowing from $k=3$ to 2.[19] Potentials with complex couplings have also been considered.[20]

We are interested in the phase structure of the one-matrix model defined by the partition function

$$Z \equiv e^{-N^2\Gamma} = \int d\Phi\, e^{-N \operatorname{tr} U(\Phi)} ,$$

where Φ is an $N \times N$ Hermitian matrix and

$$U = U_{2L}(\phi) = \sum_{j=1}^{L} \frac{1}{2j} \lambda_j \phi^{2j} ,$$

λ_j real. In this paper we will restrict ourselves to solutions that preserve the $\phi \to -\phi$ symmetry of U. (Symmetry-breaking solutions will be discussed elsewhere.) Unless otherwise stated, we consider $\lambda_L > 0$ so that U is bounded from below and the partition function Z well defined.

In the usual large-N limit (the tree level), the model is completely described in terms of the density of eigenvalues $\rho(z) \equiv (1/N) \sum_{i=1}^{N} \delta(z - x_i)$, where $(x_1, x_2, \ldots, x_N)$ is the large-N saddle-point configuration of eigenvalues of Φ that dominates the integral after the SU(N) degrees of freedom have been integrated out.[4] If all couplings λ_j are positive, $U(\phi)$ has a unique minimum at $\phi = 0$. The saddle-point solution for ρ then has a single finite band centered at the origin on which ρ has support. If, on the other hand, some λ_j, $1 \le j \le L-1$, are allowed to take on negative values, U acquires multiple local minima, and then $\rho(z)$ can have support in more than one band. This phenomenon was first observed and studied in unitary matrix models for QCD[21] and also more recently in the present context.[22] The various phases of the model can be characterized by the number of bands on which ρ has support; it is the case that, as a function of the couplings, Γ is in general a different analytic function for phases with different numbers of bands. In Sec. II we discuss the phase structure for U_6, obtaining the phase boundaries of the one-, two-, and three-band phases that are possible for this potential. For completeness and use in later sections, we also reproduce the known phase diagram for U_4. The phase diagram is determined using the Schwinger-Dyson equation[23,24] satisfied by the generating function of monomial expectation values

$$F(z) \equiv \frac{1}{N} \left\langle \operatorname{tr} \frac{1}{z - \Phi} \right\rangle ,$$

which is related to ρ. In Sec. II we spend some time distinguishing two types of critical lines that can arise and mention the ones that are relevant for double scaling. We also determine the critical exponents at the various phase boundaries for U_6.

Nonperturbative solutions of the matrix model have been obtained at specific subspaces of the coupling-constant space where the susceptibility develops a singularity, using the method of orthogonal polynomials.[25–27] Singularities that admit of a double-scaling limit, and hence such solutions, are possible typically at the edge of a phase in matrix models. If a particular phase boundary is a boundary of two distinct phases, the nature of the singularity and hence the double-scaling limit if it exists, as well as the solution, depend upon the phase from which the boundary is approached, because the susceptibility is a different analytic function of the couplings in the two phases. The solutions obtained in Ref. 7 are valid at the boundaries of the one-band phase and only when these boundaries are approached from the one-band side. The reason for this limitation is that in the continuum (large-N) limit in which the solutions have been obtained, the orthogonal polynomial recursion coefficients R_n have been assumed to approach a single function $R(x)$ ($x = n/N$). It turns out that this simple continuum limit of the R_n's is valid only within the one-band phase. As we will show in this paper, in multiband phases R_n do not approach a single function in this limit, and one has to generalize appropriately the *Ansatz* to obtain solutions from multiband phases.

Strictly speaking, the R_n approach a single function $R(x)$ in the continuum limit only when U has one minimum. For the region in which U has two minima, it has been suggested[28] that a "period-2" *Ansatz* for the continuum limit of the R_n's be used: R_n for n even approach a function $A(x)$ in the continuum limit and R_n for n odd approach a different function $B(x)$. When U has three or more minima, which is the case for the simplest model we wish to study, U_6, the continuum limit has not been investigated before.

We investigate the pattern of the continuum limit of the recursion coefficients in Secs. III–V both numerically and analytically when U has one to three minima. Our numerical results support the period-1 and -2 continuum limits when U has, respectively, one and two minima and, further, when U has three minima, provide evidence for a periodicity of 3.

To understand these results analytically and to explain the band structure from a given periodicity in the R_n, in Sec. III we relate the R_n's to the tree-level generating function $F(z)$, in terms of which the band structure is explicit. To do this we employ the operator formalism[27,29] where $F(z) \equiv (1/N) \sum_n \langle n | (z - \hat{\phi})^{-1} | n \rangle$, and $\hat{\phi}$ in turn is an operator whose matrix elements depend upon the R_n. Concentrating on the period-2 *Ansatz*, we show that it correctly reproduces the phase boundary between the one- and two-band phases, and leads to the correct solution on either side of the phase boundary.

In Sec. IV we discuss the double-scaling limit at a boundary of the two-band phase using the period-2 *Ansatz* and show how the double-scaling procedure gives rise to both the equation that describes the boundary as well as the nonperturbative solution at the boundary. For U_4 and U_6 the phase boundary is characterized by the critical exponent $k = 1$, and the result is given in terms of a solution of the Painlevé II equation. (The result for U_4 was also mentioned in Ref. 19.) In the same section we obtain a $k = 2$ nonperturbative solution for the two-band phase. This occurs on a one-dimensional curve in the four-dimensional coupling-constant space of the potential U_8. This solution satisfies an equation ($k = 2$) of the modified Korteweg–de Vries (KdV) hierarchy. Both the solutions obtained from the two-band phase have appeared in the context of unitary matrix models.[30] The $k = 2$ solution also appears when the U_8 potential is unbounded from below.

We give a general expression for $F(z)$ in terms of a period-q *Ansatz* for the R_n's in Sec. V. The period-3 *Ansatz* is used to obtain $F(z)$ for the three-band phase in U_6. Surprisingly, we find that the result for $F(z)$ agrees with

the solution of the large-N Schwinger-Dyson equation only for the case where U_6 has three degenerate minima, which is characterized by a special surface in the coupling-constant space. A double-scaling limit, which corresponds to approaching the boundary between one- and three-band phases along this surface from the three-band side, is identified using a specific form of the period-3 *Ansatz*. We find that the nonperturbative solution using this *Ansatz* for the three-band phase at this particular point is again characterized by the $k=1$ Painlevé II equation.

Finally, in Sec. VI we conclude with a review of the status of the $k=2$ solution and mention some open questions.

II. PHASE DIAGRAM

The phase diagram indicates the region of coupling-constant space where different types of solutions for ρ characterized by the number of bands on which ρ has support are present. The solutions for ρ satisfy the saddle-point equation

$$U'(z)-2P\int dz'\frac{\rho(z')}{z-z'}=0 \tag{2.1}$$

(P stands for the principal part), which is obtained by minimizing the free energy

$$\Gamma=\Gamma_1+\Gamma_2+\Gamma_3\ , \tag{2.2}$$

where $\Gamma_1\equiv\int dz\,\rho(z)U(z)$ is the "potential term,"

$$\Gamma_2\equiv-\int\int_{z\neq z'}dz\,dz'\rho(z)\ln|z-z'|\rho(z')$$

is the "repulsion term," and $\Gamma_3\equiv\gamma[\int dz\,\rho(z)-1]$ is an additional term involving the "chemical potential" γ to enforce the constraint $\int dz\,\rho(z)=1$.

The phase structure is displayed in Fig. 1(a) for the quartic potential

$$U_4(\phi)=\frac{\mu}{2}\phi^2+\frac{g}{4}\phi^4\ ,$$

and in Fig. 1(b) schematically for the potential

$$U_6(\phi)=\frac{\mu}{2}\phi^2+\frac{g}{4}\phi^4+\frac{\lambda}{6}\phi^6$$

(derivation to be discussed shortly). Broadly speaking, when U has one minimum, one has the one-band phase; in most of the region where it has two minima, one has the two-band phase; and the three-band phase exists mostly in the region where U has three minima. The correspondence is not exact because of the repulsion term. For example, some insight into why the one-band phase extends into regions where U has more than one minima can be gained by considering the situation when all the couplings are very small. The picture in this limit is as if there is one big well whose profile is determined by the $\lambda_L\Phi^{2L}$ term, containing a number of small wells whose number and location depend upon the signs and magnitudes of the other couplings. Because of the repulsion energy, the eigenvalues do not see the fine structure at the bottom of the well, but distribute themselves into a single band seeing only the outer walls of the big well. The equations for the curves a, b, and c in Figs. 1(a) and 1(b) and the points α,γ will be discussed shortly. Note that all three phases meet at α, which is in the region where U has two minima.

At this stage it is worth pointing out a feature of the U_6 phase diagram that is not shared by the quartic case. For U_4 the one-band phase exists above the line a whose equation is[31] $\mu=-2\sqrt{g}$ and the two-band phase exists on a and below. The existence domains of the one- and two-band phases do not overlap, but are separated by the line a. The free energy is continuous across this line. However, for U_6 it turns out that in some regions of phase space one can have more than one kind of solution of the saddle-point Eq. (2.1) for ρ; e.g., in some regions one can have simultaneously both one- and three-band solutions or simultaneously both two- and three-band solutions. When such an overlap appears, one or the other solution has the lowest free energy and is the *dominant* large-N solution, the others being *subdominant*. In Fig. 1(b) the region between two dotted lines is the one where the three-band phase has the minimum free energy. [A one-band-type solution to (2.1) exists below the upper dotted line, and a two-band solution exists above the lower dotted line, but they have higher free energy in

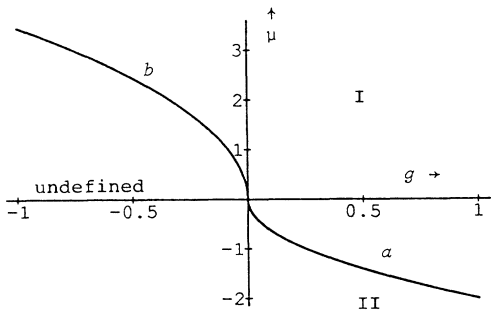

(a)

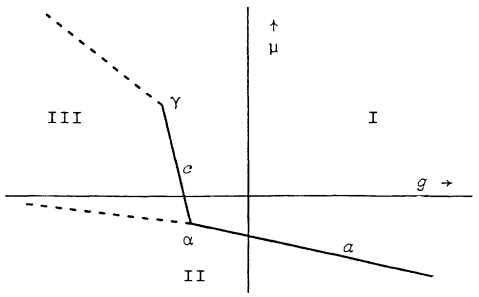

(b)

FIG. 1. (a) Phase diagram for U_4. I and II correspond to regions where one- and two-band phases exist. (b) Schematic phase diagram for U_6 in the plane $\lambda=\text{const}>0$. The lines demarcate regions where the one-, two-, and three-band phases, denoted I, II, and III, respectively, minimize the free energy.

those regions; hence, in Fig. 1(b), that region is marked as III.]

Thus it is important to distinguish between two types of boundaries on the phase diagrams. We will reserve the term *phase boundary* for those lines which demarcate the existence domain of a particular kind of phase. A particular type of solution to (2.1), e.g., a one- or two-band-type solution, comes to an end at its phase boundary; no such solution is possible beyond it. Such boundaries are shown by solid lines in the phase diagrams. For example, the line a in Figs. 1(a) and 1(b) is a phase boundary that marks the edges of both the one- and two-band phases: the former existing above and the latter on and below a. The other kind of boundaries will be called *transition lines*. They are shown by dotted lines and represent the lines across which there is a transition in the type of phase that is dominant, i.e., has the lowest free energy. Two different phases are dominant on opposite sides of a transition line; e.g., the one-band phase is dominant above the upper dotted line in Fig. 1(b) and the three-band phase is dominant below it. Note that above line a the one-band phase is by definition dominant (since no other phase exists there) and the two-band phase is dominant below it; hence a is also a transition line (in addition to being a phase boundary). The same is true for c. In general, however, it will not be the case that all phase boundaries are also transition lines, though that happens to be the case for the lines of Figs. 1(a) and 1(b).

We will be primarily interested in the phase boundaries, because those are the regions of phase space that may possibly admit a double-scaling limit and hence a nonperturbative solution. The reason is that within the existence domain of a particular phase $\rho(z)$, and hence Γ, is an analytic function of the couplings, becoming singular at the phase boundary. Typically, this singularity is enhanced at every subsequent order in the topological $1/N$ expansion in a systematic way that allows one to take the double-scaling limit and obtain a nonperturbative solution. On the other hand, across a transition line, while there is a transition in the type of phase that is dominant at the tree level, there is typically no nonanalyticity in any given phase that would allow a systematic enhancement of higher-genus contributions necessary for double scaling and a nonperturbative solution. The phase boundaries for U_6 are plotted in Figs. 2(a)–2(c) and will be discussed below. At this point we should also remark that all the "lines" in Fig. 1(b) and Fig. 2 actually represent two-dimensional surfaces in the three-dimensional coupling space of U_6, and that the "points" α and γ represent one-dimensional curves. In general, whenever we use a phrase such as "transition line," the dimensionality of the "line" should be clear from the context.

The generating function

$$F(z)=\frac{1}{Z}\int d\Phi\, e^{-N\,\mathrm{tr}U(\Phi)}\frac{1}{N}\mathrm{tr}\frac{1}{z-\Phi}$$

satisfies the large-N Schwinger-Dyson equation[24] $F(z)^2-U'(z)F(z)+b(z)=0$, where $b(z)\equiv\sum_{m=0}^{L-1}b_m z^{2m}$, $b_m\equiv\sum_{p=0}^{L-m-1}\lambda_{p+m+1}w_{2p}$, and $w_{2p}\equiv(1/N)\langle\mathrm{tr}\Phi^{2p}\rangle$. Its solution,

$$F(z)=\tfrac{1}{2}[U'(z)+\sqrt{\Delta(z)}]\ , \tag{2.3}$$

$$\Delta(z)\equiv[U'(z)]^2-4b(z)\ , \tag{2.4}$$

must satisfy the following constraints: Equation (2.3) must have only real singularities in the complex z plane (the eigenvalues of Φ are real); it must be consistent with

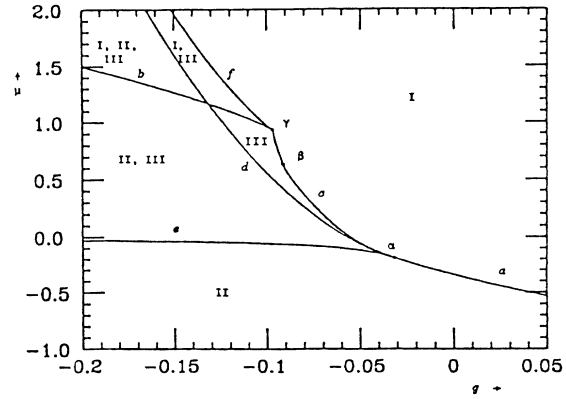

(a)

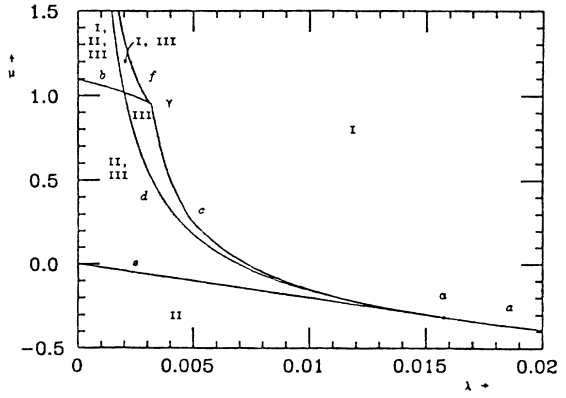

(b)

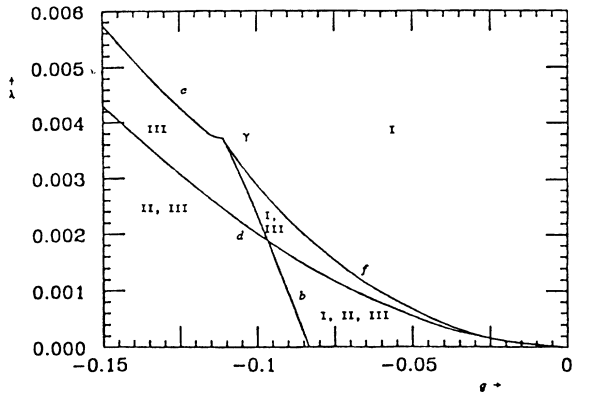

(c)

FIG. 2. (a) Phase boundaries for U_6 in the $\lambda=0.003$ plane. (b) Phase boundaries for U_6 in the $g=-0.1$ plane. (c) Phase boundaries for U_6 in the $\mu=1$ plane.

the large z expansion $F(z)=(1/z)(1+w_2/z^2+w_4/z^4+\cdots)$; and finally it must lead to a density function that is positive semidefinite for real z. In terms of $F(z)$, $\rho(z)$ for real z is given by

$$\rho(z)=-\frac{1}{2\pi}\mathrm{Im}\sqrt{\Delta(z)}\ , \tag{2.5}$$

which can be seen by comparing (2.1) with the expression $F(z)=\int dz'\rho(z')/(z-z')$.

Every odd degree zero of $\Delta(z)$, which is a $4L-2$ degree polynomial, is a branch point of $F(z)$ and, hence, must be real. Since $\Delta(z)$ changes sign across every such point as we traverse along the real axis, it follows that the branch cuts of F are the bands on which ρ has support. The positivity of ρ is a powerful constraint on the zeros of Δ, namely, that between any two adjacent square-root branch cuts of F (i.e., between any two adjacent pairs of adjacent single zeros of Δ) there must be at least one double zero of Δ. A phase with a given number of bands for a given potential can be characterized by the possible configuration of zeros of $\Delta(z)$ in the complex z plane corresponding to that phase. In Figs.. 3(a) and 3(b) we depict these configurations for the one- and two-band phases, respectively, for U_4 and in Figs. 4(a), 4(b), and 4(c) for the one-, two-, and three-band phases for U_6. The diagrams depict the complex z plane whose origin is at the center of the diagram with the real axis horizontal. Each dot represents a zero of $\Delta(z)$, a total of six for each diagram for U_4 and ten for U_6. Double dots represent double zeros, and the horizontal lines connecting single zeros depict the bands where ρ will have support. We show only those configurations which are consistent with the above-mentioned constraints and respect the $\phi\rightarrow-\phi$ symmetry of the potential.

Since the band structure is determined by the locations of single and double zeros, the phase boundaries of the various phases in the coupling-constant space can be obtained by determining the values of the couplings for which the various zeros collide. For U_4 there are two phase boundaries,[4,31] curves denoted a and b, whose configurations of zeros and the corresponding equations are shown in Table I, and which are plotted in Fig. 1(a). In the diagram representing line a, for example, the four dots in the center are meant to be coincident, representing a fourth-order zero at the origin where the two bands meet each other. For U_6 there are six phase boundaries in the $\lambda>0$ region, surfaces $a-f$, which are shown in Table II and plotted in Figs. 2(a), 2(b), and 2(c) in three different planes $\lambda=0.003$, $g=-0.1$, and $\mu=1$, respectively. The one-, two-, and three-band phases are denoted I, II, and III, respectively. For $\lambda>0$, surfaces a, b, and c are phase boundaries of I, a and d of II, and c, e, and f of III. The type of phase that can exist (irrespective of whether or not it is dominant) in every region, is indicated. Our diagrams differ from those in Refs. 15 and 16 in this respect, as also in the identification of other phase boundaries. The surfaces a,c,d,e intersect at the curve α ($g=-\mu^2$, $\lambda=-\mu^3/2$, $\mu<0$) when eight zeros of $\Delta(z)$ coalesce at the origin, and surfaces b,c,f intersect at γ ($g=-\mu^2/9$, $\lambda=\mu^3/270$, $\mu>0$) when five zeros come together at each edge of the band. α and γ meet at the origin, and all three phases meet at the curve α where U_6 has two minima. This justifies the schematic phase diagram in Fig. 1(b). The curves a and b of the quartic case are restrictions, to the $\lambda=0$ plane, of the surfaces a and b for the U_6 case. The phase boundaries g, h, and i also shown in Table II are the special cases that exist only for $\lambda<0$. They are not plotted on any figure. The one-band phase exists between g and i and the two-band phase between g and h. The model is undefined beyond h and i. These three surfaces meet at a curve δ whose equation is $g=\mu^2/3$, $\lambda=\mu^3/54$, $\mu<0$. Appendix A illustrates the calculation for c.

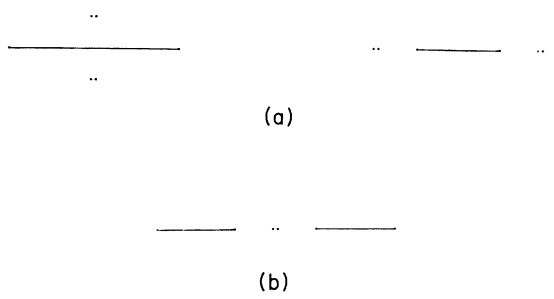

FIG. 3. (a) Configurations of zeros of $\Delta(z)$ for the one-band phase in U_4. (b) Configurations of zeros of $\Delta(z)$ for the two-band phase in U_4.

Note from Fig. 4(c) that in the interior of the three-band phase $\Delta(z)$ will have four unknowns (the four distinct zeros), but comparison with (2.4) provides only three independent equations as noted in Appendix A. Thus $F(z)$ cannot be uniquely determined from the

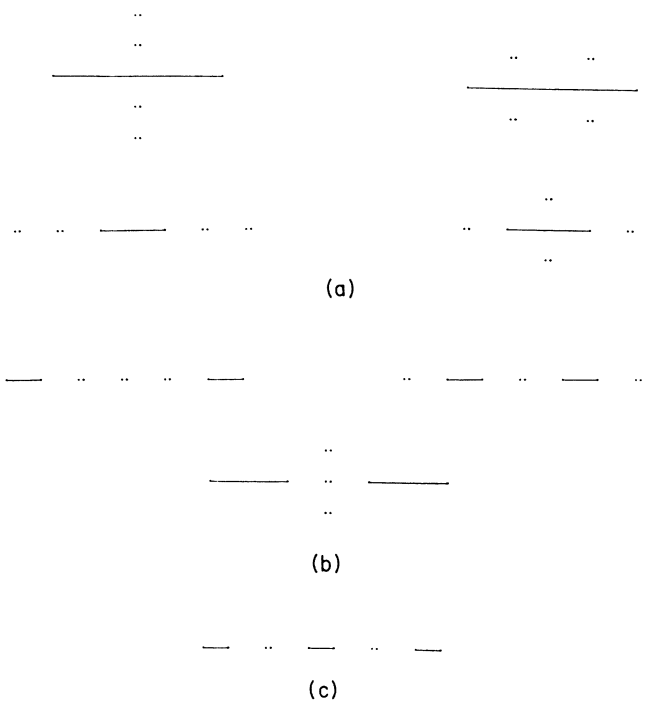

FIG. 4. (a) Configurations of zeros of $\Delta(z)$ for the one-band phase in U_6. (b) Configurations of zeros of $\Delta(z)$ for the two-band phase in U_6. (c) Configuration of zeros of $\Delta(z)$ for the three-band phase in U_6.

TABLE I. Phase boundaries for $U_4(\phi)=\frac{1}{2}\mu\phi^2+\frac{1}{4}g\phi^4$.

Name of phase boundary	Configuration of zeros of Δ corresponding to phase boundary	Equation of phase boundary
a	——..——	$\mu=-2\sqrt{g}$; $\mu<0$, $g>0$
b	..——..	$\mu=\sqrt{12\lvert g\rvert}$; $\mu>0$, $g<0$

Schwinger-Dyson equation as it stands. Equivalently, there are many saddle-point solutions $\rho(z)$ corresponding to the three-band phase that satisfy (2.1). This is because when there are three bands, the value of the chemical potential γ which appears in Γ_3 in (2.2) could be different for the central and the two sidebands. This would give the same saddle-point equation (2.1), but introduces the one extra parameter in the solutions.

One can obtain a unique three-band solution by demanding that the only admissible solution is the one for which γ is the same in all bands. However, such a requirement strongly restricts the existence domain of the three-band solutions. In Appendix A we have explicitly displayed the equations that give the generic three-band solution. The one free parameter that labels distinct solutions can be taken to be r_0, whose square root is the location of the double zero between the cuts. The demand that γ be the same in all bands fixes r_0, as discussed in Ref. 21. This constraint is conveniently expressed in the form $\int_{\sqrt{r_1}}^{\sqrt{r_2}}\sqrt{\Delta(z)}dz=0$.[16] Since $\sqrt{\Delta(z)}$ changes sign at $z=\sqrt{r_0}$, the constraint also implies that r_0 cannot be coincident with r_1 or r_2 unless $r_1=r_2$. Consequently, the existence domain of such solutions does not extend all the way down to the line e or all the way up to the line f in Fig. 2(a) because there r_0 coincides with r_1 or r_2, whereas r_1 and r_2 are unequal. The three-band solutions possible close to those lines necessarily have a different value of γ for the central and sidebands. Thus such a restriction can miss some regions of phase space where double-scaling solutions may be possible.

Finally, we turn to a calculation of the string susceptibility exponent $\gamma_{\rm str}\equiv -1/k$ based on the large-N Schwinger-Dyson equation. Given the tree-level free energy Γ as a function of the L couplings λ_j, in principle, one should identify the cosmological constant Λ as a function of the couplings and reexpress Γ in terms of Λ and an independent set of $L-1$ couplings λ_j'. Then at the phase boundary characterized by (Λ_c,λ_c'), k is defined by the formula for the susceptibility

$$\chi=\left.\frac{\partial^2\Gamma}{\partial\Lambda^2}\right|_{\lambda_c'}\sim(\Lambda-\Lambda_c)^{1/k}\ ,$$

TABLE II. Phase boundaries for $U_6(\phi)=\frac{1}{2}\mu\phi^2+\frac{1}{4}g\phi^4+\frac{1}{6}\lambda\phi^6$.

Name of phase boundary	Configuration of zeros of Δ corresponding to phase boundary	Equation of phase boundary	
a	——..——	$s=t$; $\mu<0$	
b	..——..	$u=6^{3/2}v$; $\mu>0$, $g<0$	
c	——..——..——	$u=4v$; $g<0$	only $\lambda>0$ is considered for a–f
d	——.. ..——	$w=3^{3/2}(4\lambda^2)$; $g<0$	
e	—— .... ——	$2\lambda=\mu g$; $\mu<0$, $g<0$	
f	.... ——	$u=-4v$; $\mu>0$, $g<0$	
g	.. ——..—— ..	$s=-t$; $\mu<0$, $g>0$	
h	..—— .. ——..	$w=3^{3/2}(4\lambda^2)$; $\mu<0$, $g>0$	g, h, and i exist only for $\lambda<0$
i	..——..	$u=6^{3/2}v$; $g>0$	

$s\equiv(g^2-6\mu\lambda)^{3/2}$, $t\equiv g^3-9\mu g\lambda+54\lambda^2$, $u\equiv(6g^2-20\mu\lambda)^{3/2}$,
$v\equiv -g^3+5\mu g\lambda+50\lambda^2$, $w\equiv(g^2-4\mu\lambda)^{3/2}$

where on the right-hand side we consider the most singular tree-level term as Λ approaches Λ_c. Equivalently, one can read off k from

$$\left.\frac{\partial\Gamma}{\partial\Lambda}\right|_{\lambda_c'} \sim (\Lambda-\Lambda_c)^{1+1/k} .$$

In practice, it is convenient to work with $w_2=(1/N)\langle \mathrm{tr}\phi^2\rangle=\partial\Gamma/\partial\mu$ instead of $\partial\Gamma/\partial\Lambda$, and determine k from the formula $dw_2/dt\sim t^{1/k}$, where t parametrizes a path approaching the phase boundary ($t=0$ at the boundary) in such a way that the couplings are analytic functions of t along the path.

We have found k to be equal to 1 for all phase boundaries in the $\lambda>0$ region of the phase space that we have considered [except for the already known cases of multicritical behavior, namely, the boundary b from the one-band phase ($k=2$) and γ approached from the one-band phase ($k=3$)]. When the curve α or the surfaces a or c (excluding γ) are approached from the one-band phase, or α, a, and d are approached from the two-band phase, we get $k=1$. When the curve α is approached along any of the surfaces a, c, d, or e, and the curve γ along any of the surfaces b, c, or f, also $k=1$ is obtained. For approaching phase boundaries from the interior of the three-band phase, the calculation requires making some choice out of the one-parameter family of solutions (an explicit example is discussed in Appendix B), but again we have found $k=1$ for the choices made when we approach the curve γ or the surfaces c, e, and f from the three-band phase.

$k=1$ at a particular boundary implies that the tree-level susceptibility is not singular at that boundary when approached from the phase in question. However, this does not mean that higher-genus contributions will not be singular. Typically, at phase boundaries it is seen that higher-genus contributions to the susceptibility are singular in a systematic way that allows a double-scaling limit and a nonperturbative solution. Examples of such nonperturbative solutions will be discussed in Secs. IV and V where, e.g., the two-band phase approaches a and the three-band phase approaches c, and for which, as mentioned above, we have $k=1$.

Having discussed the tree-level phase structure from the viewpoint of the Schwinger-Dyson equation, in the next section we turn to address the same question from the orthogonal polynomial method.

III. TWO-BAND PHASE USING ORTHOGONAL POLYNOMIALS

We shall discuss in this section how the generating function $F(z)$ can be obtained in the large-N spherical limit using the method of orthogonal polynomials. We recall that for each normalizable measure $d\mu(x)=\exp[-NU(x)]dx$, $-\infty<x<\infty$, a set of orthogonal polynomials $P_n(x)$ can be defined by

$$\int d\mu(x)P_n(x)P_m(x)=h_n\delta_{n,m} .$$

$P_n(x)$ is an nth-order polynomial, conventionally normalized so that the coefficient of the x^n term equals unity. For even potentials, $P_n(-x)=(-1)^nP_n(x)$, and they satisfy a two-term recursion relation: $xP_n(x)=P_{n+1}(x)+R_nP_{n-1}(x)$, with $R_0\equiv 0$. The free energy of an $N\times N$ matrix model can be expressed in terms of R_n as

$$\Gamma\equiv -N^{-2}\ln Z_N\sim \mathrm{const}-N^{-2}\sum_{n=1}^{N-1}(N-n)\ln R_n . \quad (3.1)$$

It is convenient to use the operator formalism which introduces an orthonormal basis $\{|n\rangle, n=0,1,2,\ldots\}$, each basis vector $|n\rangle$ being associated with a normalized orthogonal polynomial $P_n(x)/\sqrt{h_n}$. For instance, the recursion relation for $P_n(x)$ is equivalent to the existence of an operator $\hat{\phi}$, with matrix elements given by

$$\langle n|\hat{\phi}|m\rangle=\delta_{n,m+1}\sqrt{R_n}+\delta_{n,m-1}\sqrt{R_m} . \quad (3.2)$$

The generating function $F(z)\equiv(1/N)\langle \mathrm{tr}(z-\Phi)^{-1}\rangle$ of the original matrix model can now be expressed in terms of $\hat{\phi}$:

$$F(z)=\frac{1}{N}\sum_{n=0}^{N-1}\langle n|(z-\hat{\phi})^{-1}|n\rangle . \quad (3.3)$$

Given a potential $U_{2L}(\phi)$, the set R_n obeys a recursion relation which can be obtained by evaluating the $(n-1,n)$ matrix element of the differential operator $\partial/\partial\phi$. Upon integrating by parts, this relation, in an operator form, reads

$$n=N\sqrt{R_n}\langle n-1|U_{2L}'(\hat{\phi})|n\rangle , \quad (3.4)$$

where the right-hand side involves R_j, $n-L+1\le j\le n+L-1$. For example, in the case of $L=2$, we have the familiar relation

$$n=NR_n[\mu+g(R_{n-1}+R_n+R_{n+1})] . \quad (3.5)$$

For general L, explicit formulas can be worked out using the graphical technique of Ref. 27.

Equation (3.4) can be considered as a $(2L-1)$-term recursion relation, which allows us to find R_n iteratively, once $R_1,\ldots,R_{2L-3}$ are specified. Alternatively, for the large-N limit, one can directly analyze Eq. (3.4) once an *Ansatz* for the continuum structure of R_n as a function of $x=n/N$ is made. We first discuss our numerical calculation of R_n, whose results are displayed in Figs. 5–7. The figures cover, respectively, the cases when the potential has one, two, or three minima. The R_n's were obtained by calculating the first few numerically (R_1 for U_4 and R_1,R_2,R_3 for U_6) and using the recurrence relation (3.4) for the rest. The integrations involved in R_1,R_2,R_3 (Ref. 26) were performed using the numerical integration package of Mathematica™.

The figures suggest the kind of continuum limit that may be appropriate for the various regions of phase space. When U has one minimum, Fig. 5 suggests that R_n approach a single function $R(x)$ ($x\equiv n/N$). Figure 6 suggests that when U has two minima odd and even R_n, each approach a different continuum function for x less than a certain value, after which they become identical. Figure 7 is evidence that when U has three minima, R_n corresponding to $n=3p$, $n=3p+1$, and

$n=3p+2$ ($p=0,1,2,\ldots$) approach different continuum functions which merge at sufficiently large x. Thus the continuum limit seems to be characterized by a certain periodicity structure in n that depends upon the region of the coupling-constant space: period 1 when U has one minimum, period 2 when U has two, and period 3 when U has three minima. (Of course, since this is a numerical result, one can only say from this evidence of what the periodicity is a multiple. For example, it does not rule out the possibility that for the three-minima region the periodicity is some multiple of three, and that for the couplings for which the numerical calculation was done, the fourth branch is sufficiently close to the first, the fifth to the second, etc., for the difference to have been missed by the numerical calculation. However, the result does rule out the possibility of a periodicity 1,2,4,5,7,8,. . . at those points. Another related remark is that the numerical results are obtained only at specific points in the phase space. They do not rule out the possibility that, e.g., in another part of the three-minima region of phase space, the periodicity is different from 3.)

Note that there is no one-to-one correspondence between the periodicity and the number of bands. For example, in Fig. 6(b) the coupling constants correspond to the one-band phase, but we have period 2 for the R_n's. We have also checked at a number of points of the phase space (diagram not displayed) which are in the one-band phase, but where U_6 has three minima, for which one again gets a periodicity of 3. Thus the relationship between the periodicity and the phase structure is not *a priori* clear. In what follows we will directly analyze the band structure from (3.4) for various different *Ansätze* for the continuum structure of R_n (i.e., for various periodicities). We will see that the increased periodicity when the potential has multiple minima is crucial for understanding the multiple-band phases and the phase boundaries of the matrix model, and for obtaining nonperturbative solutions.

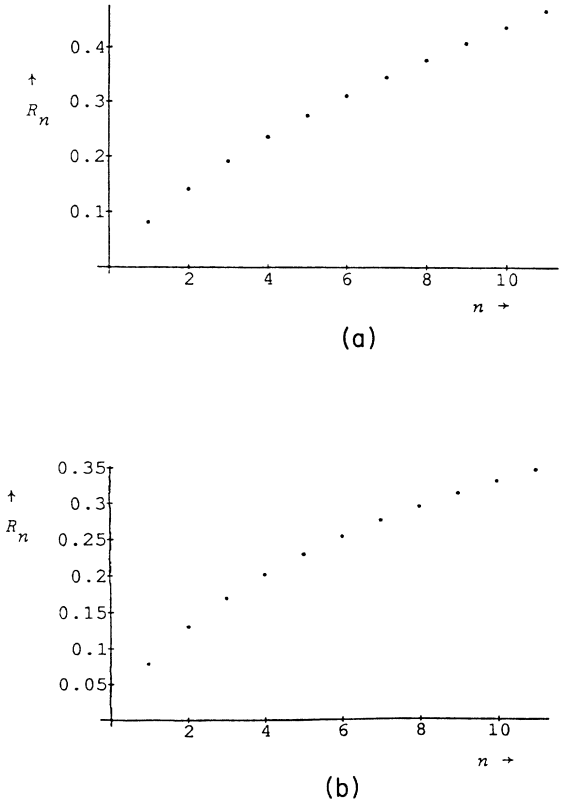

FIG. 5. (a) Numerical result for R_n when U_4 has one minimum ($N=10$, $\mu=1$, $g=1$). (b) Numerical result for R_n when U_6 has one minimum ($N=10$, $\mu=1$, $g=1$, $\lambda=1$).

A. Scalar *Ansatz* and single-band structure

The simplest continuum *Ansatz* one can make is one in which the R_n approach a single continuous function

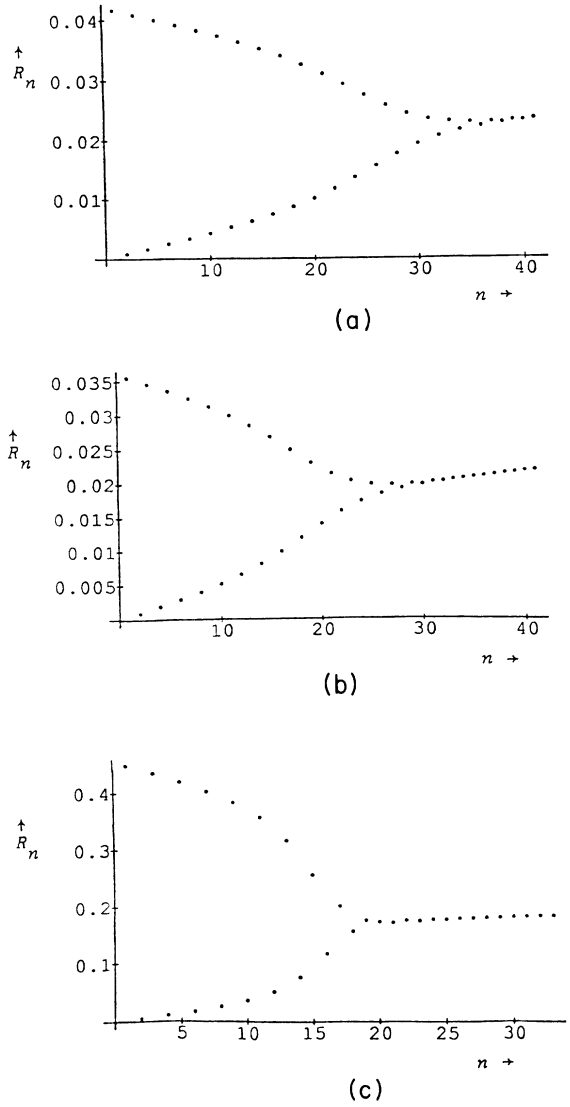

FIG. 6. (a) Numerical result for R_n when U_4 has two minima ($N=25$, $\mu=-105$, $g=2500$) and in the interior of the two-band phase. (b) Numerical result for R_n when U_4 has two minima ($N=25$, $\mu=-90$, $g=2500$) and in the interior of the one-band phase. Note that the odd and even branches merge sooner than in (a). (c) Numerical result for R_n and U_6 has two minima ($N=15$, $\mu=-6$, $g=-36$, $\lambda=108$).

$R(x)$. This will be referred to as a scalar *Ansatz* (or period 1).

In the large-N limit, Eq. (3.4) then gives

$$x = W_L(R(x)) , \tag{3.6}$$

which can be solved for $R(x)$ analytically. $W_L(R)$ is an Lth-degree polynomial, which can be obtained from $U_{2L}(\phi)$ either by the graphical method of Ref. 27 or, more compactly, using the relation $W_L(R) = \oint (du/2\pi i) U'_{2L}(u + Ru^{-1})$. For symmetric potentials whose coupling constants are all positive, a unique real solution $R(x)$ exists which is monotonically increasing over the positive x axis with $R(0)=0$. We shall refer to this class of symmetric potentials as "positive" and shall concentrate on this special class first.

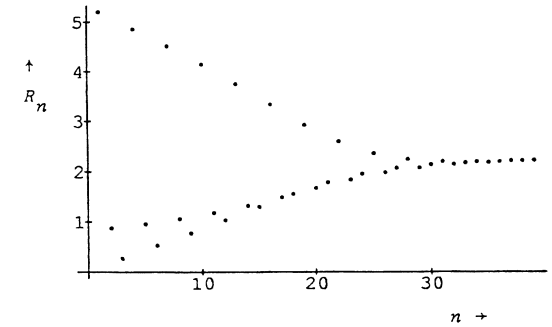

(a)

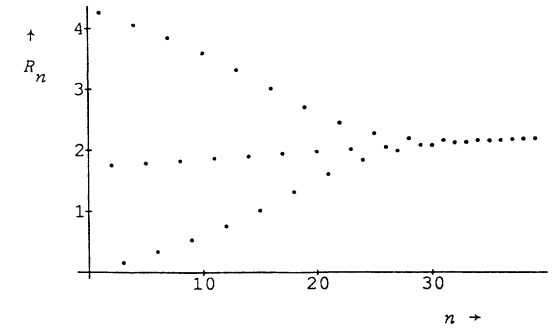

(b)

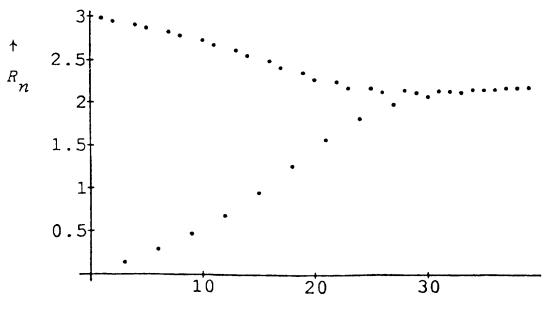

(c)

FIG. 7. (a) Numerical result for R_n when U_6 has three minima ($N=20$, $\mu=1.5$, $g=-1.010$, $\lambda=0.125$) and in the interior of the three-band phase. (b) Numerical result for R_n when U_6 has three minima ($N=20$, $\mu=1.5$, $g=-1.005$, $\lambda=0.125$) and in the interior of the three-band phase. (c) Numerical result for R_n when U_6 has three minima ($N=20$, $\mu=1.5$, $g=-1.000$, $\lambda=0.125$). This is at the boundary c of the one- and three-band phases. Further, the three minima of U_6 are degenerate at this point.

It is convenient to approach the large-N limit by using the pair of conjugate operators $\hat{l}$ and $\hat{\theta}$, where $\hat{l}|n\rangle = x_n|n\rangle$, $x_n \equiv n/N$, and $[\hat{\theta},\hat{l}] = i/N$. Under the scalar *Ansatz*, the operator $\hat{\phi}$ can be expressed as $\hat{\phi} = \sqrt{R(\hat{l})}e^{i\hat{\theta}} + e^{-i\hat{\theta}}\sqrt{R(\hat{l})}$. In the θ basis, an operator-valued function of $\hat{\phi}$ becomes a local differential operator with $\hat{l} \to -(i/N)(d/d\theta)$, and wave functions are periodic in θ with a period 2π. Since $[\hat{\theta},\hat{l}] \to 0$ as $N \to \infty$, one finds, for the diagonal matrix elements of the resolvent operator,

$$\langle n|(z-\hat{\phi})^{-1}|n\rangle \to \int_0^{2\pi} \frac{d\theta}{2\pi} [z - \phi(x,\theta)]^{-1} ,$$

where $\phi(x,\theta) = (e^{i\theta} + e^{-i\theta})\sqrt{R(x)}$. It follows that, in the large-N limit, the generating function approaches

$$F^{(1)}(z) = \int_0^1 dx \int_0^{2\pi} \frac{d\theta}{2\pi} \frac{1}{z - \phi(x,\theta)}$$

$$= \int_0^1 dx \frac{1}{\sqrt{z^2 - 4R(x)}} , \tag{3.7}$$

where the superscript signifies that (3.7) is derived under a scalar *Ansatz*.

Since $R(x)$ is bounded for $0 \le x \le 1$, Eq. (3.7) defines an analytic function for $|z|$ sufficiently large. Since $R(0)=0$ and $R(x)$ is monotonic, it follows that $F^{(1)}(z)$ is real analytic with a pair of symmetric square-root branch points located at $\pm z_1, z_1 \equiv 2\sqrt{R(1)}$. That is, (3.7) represents a single-band structure. Furthermore, since $F^{(1)}(z) \to 1/z$ as $|z| \to \infty$, it automatically leads to a properly normalized spectral density $\rho(z)$ on the cut.

Two necessary conditions for (3.7) to be a bona fide solution to the Schwinger-Dyson equation are that, on the cut, the real part of the generating function be given by $\mathrm{Re}F^{(1)}(z) = \frac{1}{2}U'(z)$ and the spectral density $\rho(z) = -(1/\pi)\mathrm{Im}F(z)$ should be non-negative. To see that this is indeed the case for the class of "positive" potentials, change the integration variable from x to $r = R(x)$ in Eq. (3.7), which yields

$$F^{(1)}(z) = \int_0^{R(1)} dr \frac{W'(r)}{(z^2 - 4r)^{1/2}} . \tag{3.8}$$

Since $W'(r)$ is real, for a fixed value of z in the range $|z| < z_1 = 2\sqrt{R(1)}$, only the region $0 \le r \le z^2/4$ contributes to $\mathrm{Re}F^{(1)}(z)$. If we again change the integration variable from r to v, $r \equiv v(1-v)z^2$, one finds $\mathrm{Re}F^{(1)}(z) = z\int_0^{1/2} dv\, W'[v(1-v)z^2]$. On the other hand, the defining relation $W_L(R) = \oint (du/2\pi i) U'_{2L}(u + Ru^{-1})$ can be inverted to give $U(\phi) = \int_0^1 (dv/v) W[v(1-v)\phi^2]$, which implies

$$U'(\phi) = 2\phi \int_0^1 dv (1-v) W'[v(1-v)\phi^2] .$$

It follows that $\mathrm{Re}F^{(1)}(z) = \frac{1}{2}U'(z)$, as required. Similarly, for the imaginary part one gets

$$\rho(z)=\frac{1}{2\pi}\int_0^{(z_1^2-z^2)/4}\frac{dr}{\sqrt{r}}W'\left[r+\frac{z^2}{4}\right], \tag{3.9}$$

and since $W'(r)>0$ for positive potentials, $\rho(z)$ automatically satisfies the positivity requirement on the cut.

The quartic potential $U_4(\phi)=\frac{1}{2}\mu\phi^2+\frac{1}{4}g\phi^4$, with $\mu\geq 0$, $g\geq 0$, provides an explicit illustration. With $W_2(R)=\mu R+3gR^2$, (3.6) leads to two solutions $R_\pm(x)=[-\mu\pm(\mu^2+12gx)^{1/2}]/6g$. Of the two, only $R_+(x)$ satisfies the requirement that $R(x)>0$ for $0\leq x\leq 1$, which leads to a well-defined monotonically increasing function satisfying the condition $R(0)=0$. Equation (3.9) leads to $\rho(z)=(g/2\pi)(z^2-z_0^2)(z_1^2-z^2)^{1/2}$, where $z_1^2=4R_+(1)>0$ and $z_0^2=-2[\mu/g+2R_+(1)]<0$, in agreement with Ref. 4. In general, for a positive symmetric polynomial potential of order $2L$, (3.9) can be evaluated easily, leading to a spectral density $\rho(z)=\mathcal{P}_L(z^2)(z_1^2-z^2)^{1/2}$, where $\mathcal{P}_L(z^2)$ is a $(L-1)$th-order polynomial in z^2, positive over the region $0\leq|z|\leq z_1$. This shows that the scalar *Ansatz* is indeed appropriate for positive potentials. Furthermore, since the above $\rho(z)$ always leads to regular one-point functions, we conclude that no "double-scaling" limit can arise in this case.

What will happen for potentials with negative couplings? For instance, for the quartic potential with $\mu<0$ and $g>0$, of the two solutions of (3.6), once again $R_+(x)$ satisfies the requirement that $R(x)>0$ for $0\leq x\leq 1$. Unfortunately, the condition $R(0)=0$ can no longer be satisfied, and one can explicitly demonstrate that Eq. (3.7) no longer represents a solution of the Schwinger-Dyson equation. The situation gets worse if $g<0$. First of all, the original measure for our orthogonal polynomials is no longer normalizable, and one can no longer be assured of obtaining a real solution for $R(x)$ for x positive. For a general potential with some negative couplings, one might be faced with a function $R(x)$ which is discontinuous over the range $0\leq x\leq 1$. It is also possible that a real continuous $R(x)$ exists for $0\leq x\leq 1$, but the condition $R(0)=0$ is no longer satisfied. For all these situations, Eq. (3.7) no longer corresponds to a solution of the Schwinger-Dyson equation and the single-component scalar *Ansatz* for the large-N limit of R_n is inapplicable.

A possible alternative approach is to always start with a positive potential and then analytically continue $F^{(1)}(z)$ into regions involving negative couplings. Indeed, (3.8) provides such a continuation. In terms of this representation, $F^{(1)}(z)$ always satisfies the Schwinger-Dyson equation, provided that the upper limit of the integral, $R(1)$, is real and well defined. It also automatically leads to the single-band spectral density above. It is clear from (3.8) that one can analytically continue from the region of positive couplings to a much larger region even if W' turns negative.

However, this continuation process can be stopped by the following obstacles: $R(1)$ can start to turn complex or take a discontinuous jump. This always happens if we continue into the region where the potential becomes unbounded from below, e.g., the region $\mu>0$ and $g<0$ for a quartic potential. [The inevitability of this outcome can easily be seen as follows. Note that, in going from Eq. (3.4) to Eq. (3.6), the N dependence has disappeared. Since (3.4) is linear in coupling constants λ_j, it follows that

$$R(\alpha x,\alpha\lambda_j)=R(x,\lambda_j), \tag{3.10}$$

where we have explicitly exhibited the dependence of $R(x)$ on coupling constants. For a quartic potential with $g<0$ and $\mu>0$, no real solution can exist for x sufficiently large. It follows that one can always decrease $|g|$ and μ with g/μ fixed so that $R(1)$ becomes complex. Indeed, this is precisely the condition for developing the standard $k=2$ double-scaling limit, which corresponds to the curve b depicted in Table I and Fig. 1(a).] Another obstacle is that $\mathcal{P}_k(z^2)$, and hence the spectral density, can turn negative over the branch cut, while $R(1)$ remains well defined. This invariably occurs when the potential develops multiple local minima while remaining bounded from below. For U_4 this happens at the line a, which marks the phase boundary between the one- and two-band phases.

B. Two-component *Ansatz* and double-band structure

If one wants to deal directly with potentials involving negative couplings, it is clear that one is forced to go beyond the scalar *Ansatz*. We now consider the period-2 *Ansatz*, namely, that in the large-N limit $R_n\to A(x)$ for n even and $R_n\to B(x)$ for n odd, where $x=n/N$. We will first concentrate on the "kinematic" aspects of this two-component *Ansatz* before turning to the question of its consistency and its applicability.

Since $\hat{\phi}$ connects only the "nearest-neighbor" even-odd and odd-even basis states, it is convenient to think of the Hilbert space as a direct sum of an "even space" and an "odd space," i.e., $\mathcal{H}=\mathcal{H}_0\oplus\mathcal{H}_1$, where $\mathcal{H}_\sigma$ is spanned by basis states $\{|n\rangle,\ n=2p+\sigma,\ p=0,1,2,\ldots\}$. One can then arrange $\hat{\phi}$ into a 2×2 matrix form where $\hat{\phi}_{\sigma,\sigma'}$ maps $\mathcal{H}_{\sigma'}\to\mathcal{H}_\sigma$. For the period-2 *Ansatz*, one finds that $\hat{\phi}_{0,0}=\hat{\phi}_{1,1}=0$, $\hat{\phi}_{1,0}=e^{-i\hat{\theta}}\sqrt{B(\hat{I})}+\sqrt{A(\hat{I})}e^{i\hat{\theta}}$, and $\hat{\phi}_{0,1}=e^{-i\hat{\theta}}\sqrt{A(\hat{I})}+\sqrt{B(\hat{I})}e^{i\hat{\theta}}$. Similarly, any operator-valued function of $\hat{\phi}$ can also be arranged in a 2×2 matrix form, defined by a power-series expansion in $\hat{\phi}$. In particular, the resolvent operator $\hat{G}=(z-\hat{\phi})^{-1}$ now has four components $\hat{G}_{\sigma,\sigma'}$. In the large-N limit where $[\hat{I},\hat{\theta}]\to 0$, one finds that the diagonal matrix element $\langle n|(z-\hat{\phi})^{-1}|n\rangle\equiv\langle 2p+\sigma|(z-\hat{\phi})^{-1}|2p+\sigma\rangle$ approaches the limit $\int_0^{2\pi}(d\theta/2\pi)G_{\sigma,\sigma}(x,\theta)$, where $G(x,\theta)=[z-\phi(x,\theta)]^{-1}$ is an ordinary 2×2 matrix function with

$$\phi(x,\theta)=\begin{bmatrix}0 & \sqrt{A(x)}e^{-i\theta}+\sqrt{B(x)}e^{i\theta}\\ \sqrt{B(x)}e^{-i\theta}+\sqrt{A(x)}e^{i\theta} & 0\end{bmatrix}. \tag{3.11}$$

It immediately follows from (3.3) that in the large-N limit the generating function approaches

$$F(z)=\frac{1}{2}\int_0^1 dx \int_0^{2\pi}\frac{d\theta}{2\pi}\frac{2z}{z^2-A(x)-B(x)-\sqrt{A(x)B(x)}(e^{2i\theta}+e^{-2i\theta})} . \tag{3.12}$$

The factor of $\frac{1}{2}$ comes from the conversion of the sum over p, ($n=2p+\sigma$) to an integral over x, and the factor $2z$ under the integral comes from the trace over $\sigma=0,1$. A contour integration immediately yields a general representation for the generating function under a two-component *Ansatz:*

$$F^{(2)}(z)=z\int_0^1 dx\frac{1}{\{[z^2-\eta(x)]^2-4\xi(x)\}^{1/2}} , \tag{3.13}$$

where we have added a superscript for $F(z)$. Instead of using $A(x)$ and $B(x)$, we have also expressed (3.13) in terms of symmetric combinations $\eta(x)\equiv A(x)+B(x)$ and $\xi(x)\equiv A(x)B(x)$. As a consistency check, we note that (3.13) reduces to (3.7) if $A(x)=B(x)=R(x)$.

We now ask, under what conditions is the period-2 *Ansatz* valid? The answer verifies our expectation from the numerical calculation and from the fact that the scalar *Ansatz* applies for positive potentials, that the period-2 *Ansatz* is valid when the potential has two minima. To be explicit, let us first concentrate on U_4. We will show that the period-2 structure describes both the one- and two-band phases in the $\mu<0$, $g>0$ region and reproduces the correct phase boundary and solution of the Schwinger-Dyson equation. Starting with (3.5), the spherical limit immediately leads to two coupled equations:

$$\begin{aligned} x&=\mu A(x)+gA(x)[A(x)+2B(x)] ,\\ x&=\mu B(x)+gB(x)[B(x)+2A(x)] . \end{aligned} \tag{3.14}$$

The sum and difference of these equations lead to

$$\begin{aligned} 2x&=(A+B)[\mu+g(A+B)]+gAB ,\\ 0&=(A-B)[\mu+g(A+B)] . \end{aligned} \tag{3.15}$$

If we assume $A(x)\neq B(x)$, the difference equation implies that $\eta(x)=-\mu/g$. Since A and B must be positive, this means $\mu<0$ (we are considering $g>0$). Further, $\xi(x)=x/g$; hence,

$$(A-B)^2=\frac{\mu^2}{g}-4x . \tag{3.16}$$

Since the left-hand side cannot be negative and the right-hand side turns negative for x large and positive, the assumption that $A(x)\neq B(x)$ must break down for large x. One concludes that $A(x)$ must equal $B(x)$ for $x\geq\bar{x}$, $\bar{x}\equiv\mu^2/4g$. Thus we have shown that the period-2 *Ansatz* is valid only when U_4 has two minima and for the range $0\leq x<\bar{x}$. [We note at this stage that the tendency of odd and even recursion coefficients to merge earlier as one decreases $\bar{x}$ is also visible at finite N numerically in Figs. 6(a) and 6(b).]

The question that remains is whether Eq. (3.13), which follows from this *Ansatz,* is a solution of the Schwinger-Dyson equation in this region. The one- and two-band solutions to the Schwinger-Dyson equation are exhibited in Eqs. (A6) and (A8), respectively. To see that they are both reproduced from this *Ansatz,* first consider the case where $\bar{x}>1$ so that $A(x)\neq B(x)$ in the entire integration range. With $\eta(x)=-\mu/g$, $\xi(x)=x/g$, the x integration can be carried out trivially, leading, for $z=|z|+i\epsilon$, to $F^{(2)}(z)=\frac{1}{2}U_4'(z)-i\pi\rho(z)$, where $\rho(z)$ is given by (A8). Hence we reproduce the two-band solution below the line a whose equation is given simply by $\bar{x}(\mu,g)=1$.

When $0>\mu>-2\sqrt{g}$ (i.e., $0<\bar{x}<1$), we separate the integration range in (3.13) into $[0,\bar{x}]$ and $[\bar{x},1]$. The first region contributes $\frac{1}{2}U_4'(z)-gz^2(z^2+2\mu/g)^{1/2}$. For $[\bar{x},1]$, we must use the solution $A(x)=B(x)\equiv R(x)$ of our earlier scalar *Ansatz,* so that $\eta=2R$ and $\xi=R^2$. This leads to $\int_{R(\bar{x})}^{R(1)}dr\,W'(r)/(z^2-4r)^{1/2}$. Combining the two, one finds that

$$F^{(2)}(z)=\int_0^{R(1)}dr\frac{W'(r)}{(z^2-4r)^{1/2}} .$$

This is easily integrated and yields the correct one-band spectral density (A6). Note from (3.8) that in this region $F^{(2)}(z)=F^{(1)}(z)$; i.e., the two-component *Ansatz* reproduces the earlier single-band structure obtained by an analytic continuation from the positive μ region.

A similar situation also occurs for the U_6 potential. For instance, instead of (3.15), we have

$$\begin{aligned} 2x&=\eta(\mu+g\eta+\lambda\eta^2+2\lambda\xi)+2\xi(g+2\lambda\eta) ,\\ 0&=(A-B)(\mu+g\eta+\lambda\eta^2+2\lambda\xi) . \end{aligned} \tag{3.17}$$

To illustrate the key features, let us consider a simple situation where $g=0$, $\lambda=1$. Assume that $A(x)\neq B(x)$. It follows from (3.17) that $\eta^2+\xi=-\mu$ and $2\xi\eta=x$. Since η and ξ must be positive, we first note that a two-component *Ansatz* is compatible only for $\mu<0$, as expected. However, even with μ fixed and negative, one finds by eliminating ξ that $\eta^3+\mu\eta+x=0$, which has no real positive solution for x sufficiently large. One can therefore find a value $\bar{x}$ beyond which one must have $A(x)=B(x)$. The situation is then identical to that of a quartic potential. For μ sufficiently negative so that $\bar{x}>1$, one has $A(x)\neq B(x)$ for $0\leq x\leq 1$, and $F^{(2)}(z)$ leads to a two-band structure. Conversely, as one decreases $|\mu|$ so that $\bar{x}<1$, one finds that $F^{(2)}(z)$ agrees with the analytic continuation of $F^{(1)}(z)$ from the positive potential region, which describes a single-band structure. This analysis can also be carried out for $g\neq 0$. $\bar{x}(\mu,g,\lambda)$ can be found by setting $\eta=2r$, $\xi=r^2$ into two equations derived from (3.17) for $A\neq B$ and eliminating r. The single- and double-band transition line is given by the condition $\bar{x}(\mu,g,\lambda)=1$, which is the same as the equation for line a indicated in Table II and Figs. 4(a) and 4(b).

We briefly comment on the generality of our result. Note that a relation analogous to (3.10) also applies in the period-2 case:

$$A(\alpha x,\alpha\lambda_j)=A(x,\lambda_j),\quad B(\alpha x,\alpha\lambda_j)=B(x,\lambda_j)\ . \tag{3.18}$$

For potentials bounded from below, at λ_j sufficiently small, the Coulomb repulsion energy will always overcome the potential barrier, thus leading to a single-band structure. This implies that there always exists an $\bar{x}(\lambda_j)$ such that $A(x)=B(x)\equiv R(x)$ for $x>\bar{x}$, where $R(x)$ is real and well defined. For λ_j small, $\bar{x}<1$ so that a single-band structure is obtained. By multiplying $\lambda_j\to\alpha\lambda_j$, $\alpha>1$, it is always possible to reach a situation where $\bar{x}\to\alpha\bar{x}>1$ so that a two-band structure is reached. The transition line between the single- and double-band regions is always given by the condition $\bar{x}(\lambda_j)=1$.

We close this section by pointing out that the analytic continuation of (3.8) across the curve $\bar{x}=1$ from the $\bar{x}<1$ region remains well defined. However, this continuation is unacceptable in the region $\bar{x}>1$ since the would-be single-band spectral density is no longer positive there. On the other hand, if one approaches the curve $\bar{x}=1$ from below, the double-band structure, obtained under a two-component *Ansatz*, would cease to exist at this phase boundary. In the next section we discuss the double-scaling limit and nonperturbative solution as one approaches the line $\bar{x}=1$ from the two-band side.

IV. NONPERTURBATIVE SOLUTIONS AND TWO-COMPONENT *ANSATZ*

The possibility of a nonperturbative solution to a large-N matrix model rests on the observation that, although the spherical contribution to the susceptibility χ normally dominates over that from higher genera, there exist singularities of χ such that sufficiently close to them, singular contributions from all genera are of the same order and their nonperturbative sum can be characterized as the solution of a certain differential equation. This nonperturbative "string equation" can be obtained by analyzing the recursion equation for R_n [Eq. (3.4)] in the so-called "double-scaling" limit. Extensive analyses have been carried out under the scalar *Ansatz*, where one explores the structure of $R(x)$ in an infinitisimal neighborhood of $x=1$.

In this section we discuss nonperturbative solutions at a phase boundary of the two-band phase using the period-2 *Ansatz*, where the R_n in the large-N limit approach two distinct functions $A(x)$ and $B(x)$ for n even and odd, respectively. We have learned from our spherical analysis in the last section that the line $\bar{x}(\lambda_j)=1$ is a boundary between the one- and two-band phases with the region $\bar{x}<1$ corresponding to the one-band phase and $\bar{x}>1$ to the two-band phase. We will be interested in the behavior of $A(x)$ and $B(x)$ near $x=1$ when the couplings approach the line $\bar{x}=1$ from the two-band phase, because the singular contribution to the free energy (3.1) is determined from this behavior. Since $A(x)$ and $B(x)$ are not equal for $x<\bar{x}$, it follows that to develop a double-scaling limit appropriate for approaching the singular line from the two-band phase, we must insist on having $A(x)\neq B(x)$ for $x<1$, but in such a way that as $\bar{x}$ approaches unity from above (i.e., the couplings approach the singular line), and $A(1)$ and $B(1)$ approach each other.

Let us begin by first considering the simplest situation where a two-component *Ansatz* is relevant, namely, the quartic potential $U_4(\phi)=(\mu/2)\phi^2+(g/4)\phi^4$, with $\mu<0$ and $g>0$. Let us denote R_n by A_n for n even and B_n for n odd. To go beyond the spherical limit, we must keep track of higher-order terms in $1/N$ in a simultaneous expansion about $x=1$.

As in the one-band phase, we define a scaling variable t by $x=1-\epsilon^2 t$ and, in this case, two scaling functions $f(t)$ and $h(t)$ by

$$\begin{aligned} A_{n\pm j}&=r+\epsilon^2 f(t\mp j\epsilon)+\epsilon h(t\mp j\epsilon)\quad \text{for } n\pm j \text{ even}\ ,\\ B_{n\pm j}&=r+\epsilon^2 f(t\mp j\epsilon)-\epsilon h(t\mp j\epsilon)\quad \text{for } n\pm j \text{ odd}\ , \end{aligned} \tag{4.1}$$

where $\epsilon=N^{-1/3}$. Starting from (3.5), we write down two separate equations for even and odd n, $x=n/N\sim 1-\epsilon^2 t$. In the large-N limit, one makes use of (4.1) and expands $f(t\mp j\epsilon)$ and $h(t\mp j\epsilon)$ in Taylor series around t. One could at this point set the coupling constants to take on their critical values. However, we prefer not to do so. Instead, we demonstrate that this critical line emerges as a necessary condition for the consistency of our scaling law [Eq. (4.1)] in a double-scaling analysis.

From the structure of (3.5) and from our scaling *Ansatz* (4.1), it is clear that sum of the even and odd equations contains terms with even powers in ϵ and their difference contains only terms with odd powers in ϵ. Expanding to the order ϵ, one obtains two constraints on the coupling constants:

$$3gr^2+\mu r=1,\quad 2gr+\mu=0\ . \tag{4.2}$$

By eliminating the parameter r, we find a nontrivial scaling is possible only on the single line $\mu=-2\sqrt{g}$, as expected. [Note that the signs of μ and g are uniquely determined since $r>0$ must hold. We also note that the second constraint will be absent if one assumes that $h(t)\equiv 0$, which corresponds to the scaling limit appropriate for the one-band phase. This is consistent with the fact that the susceptibility is actually nonsingular when approached from the one-band phase.]

Expanding next to the order ϵ^3 and after enforcing (4.2), one obtains two equations which determine scaling functions f and h:

$$-t=\frac{1}{r^2}(4rf-h^2),\quad 0=2fh-rh''\ . \tag{4.3}$$

After eliminating $f(t)$ and appropriately rescaling t and h, one arrives at the Painlevé II equation for $h(t)$:

$$th=h^3-\tfrac{1}{2}h''\ . \tag{4.4}$$

This string equation has been identified more naturally in a treatment for large-N unitary matrix models.

One gains a better physical understanding of the function $h(t)$ by examining the expression (3.1) for free energy in terms of R_n. One finds that in the double-scaling limit the singular part of the susceptibility $\chi(t)\equiv\Gamma''(t)$ is proportional to $h^2(t)$. The critical exponent for the susceptibility can be determined by examining the asymptotic behavior of $h(t)$ for large t; $h(t)\sim\sqrt{t}\,(1-\frac{5}{96}t^{-3/2}+\cdots)$

implies that $\chi(t)\sim t(1-\frac{5}{48}t^{-3/2}+\cdots)$. The leading term, representing the tree level, tells us that for this solution $k=1$, as is also easily determined from the tree-level analysis described in Sec. II. To distinguish (4.4) from those previously obtained under a scalar *Ansatz*, we shall refer to (4.4) as belonging to a class of "type-II" string equations.

We are now in the position to analyze the case of U_6. The tree-level analysis tells us that there is a phase boundary between the two- and one-band phases. We expect again a type-II solution as one approaches this boundary from the two-band side. Starting from the recursion relation (3.4) for U_6 and using the same scaling assumption, [Eq. (4.1)], one finds that the same Painlevé II equation (4.4) is reached if the coupling constants satisfy the two equations

$$10\lambda r^3+3gr^2+\mu r=1 ,$$
$$6\lambda r^2+2gr+\mu=0 .$$

These two equations represent a surface in the phase space. Eliminating r, we recover precisely the equation for a in Table II. We also note that the value $k=1$, to which the solution (4.4) corresponds, again agrees with the large-N analysis.

Are there nonperturbative solutions involving a two-band phase which correspond to higher values of k? Since the critical exponent of pure 2D quantum gravity is $\gamma_{\rm str}=-\frac{1}{2}$, the case of $k=2$ is of special interest. In our tree-level analysis for U_4 and U_6 with $\lambda>0$, no transition surface with a $k=2$ singularity was found when approached from a two-band phase. It is actually not difficult to directly examine the ϕ^8 potential $U_8(\phi)=\frac{1}{2}\mu\phi^2+\frac{1}{4}g\phi^4+\frac{1}{6}\lambda\phi^6+\frac{1}{8}\nu\phi^8$, for the possible existence of a $k=2$ solution using our current procedure. Starting from (3.4), we again apply the scaling law $x=1-\epsilon^4 t$, $\epsilon=N^{-1/5}$, and $R_{n\pm j}$ scaled as in (4.1). One first finds that this scaling is consistent if the coupling constants satisfy the system of equations

$$35\nu r^4+10\lambda r^3+3gr^2+\mu r=1 ,$$
$$140\nu r^3+30\lambda r^2+6gr+\mu=0 ,$$
$$30\nu r^2+6\lambda r+g=0 ,$$
$$6\nu r+\lambda=0 .$$

These equations define a line in the four-dimensional coupling-constant space, which can be parametrized as

$$\mu=-\frac{4}{3r},\quad g=-\frac{2}{r^2},\quad \lambda=\frac{2}{r^3},\quad \nu=-\frac{1}{3r^4} . \tag{4.5}$$

Two scaling functions can next be determined by the system of equations

$$\begin{aligned} r^4 t &= h^4-8rfh^2+16r^2f^2-\tfrac{8}{3}r^2(h')^2 \\ &\quad -\tfrac{8}{3}r^2hh''+\tfrac{16}{3}f'' , \\ 0 &= 8fh^3-16rf^2h-4rh(h')^2-4rh^2h'' \\ &\quad -\tfrac{16}{3}r^2f''h+\tfrac{8}{3}r^3h^{[4]} . \end{aligned} \tag{4.6}$$

Note that $f(t)$ can be eliminated easily since an identical factor involving f enters in both equations, which leads to a single equation for $h(t)$. By rescaling $t\to 2^{4/5}t$ and $h\to 2^{1/5}rh$, one finds another type-II equation for $h(t)$:

$$th=h^5-\tfrac{5}{3}h(h')^2-\tfrac{5}{3}h^2h''+\tfrac{1}{6}h^{[4]} . \tag{4.7}$$

By examining the asymptotic behavior of $h(t)$, one verifies that this solution corresponds to $k=2$. Interestingly, this $k=2$ type-II equation has again been obtained previously from unitary matrix models.[30]

At this point we remark on the structure of zeros of $\Delta(z)$ at points of the coupling-constant space where Painlevé-II-type solutions have been obtained. Note from Tables I and II that for both U_4 and U_6 at a, where we have a Painlevé-II-type solution, we have four zeros of $\Delta(z)$ merging at the origin. For the Painlevé-II-type solution (4.7), one can check again that at (4.5) a number of zeros coalesce at the origin (in this case the number of coalescing zeros is eight, due to the higher potential). This is similar to the behavior seen in the $k=1$ and 2 unitary matrix models when two ends of the arc merge. Also, for Hermitian matrix models, $k=2$ solutions (whether Painlevé I or II) seem to appear when a double zero coalesces with the single zero that forms the outside edge of the band [e.g., at the line b in Table I and II, and on the line (4.5) in U_8]. This outside edge is absent in the unitary case due to periodicity. It would be interesting to identify a general correspondence, if any, between the nonperturbative equation and the tree-level structure of the zeros, and between the latter and the critical exponent.

We end this section with a few remarks on the double-scaling solution for the two-band phase for general k. Although we do not have a general proof, we expect the following to be true. To obtain the scaling solution corresponding to a given value of k, one must start with a model in at least a $2k$-dimensional coupling-constant space, i.e., U_{4k}. The scaling law would be

$$x=1-\epsilon^{2k}t,\quad \epsilon=N^{-1/(2k+1)} , \tag{4.8}$$

with $A_{n\pm j}$, $B_{n\pm j}$ given by (4.1). This scaling will be consistent along a one-dimensional line in $2k$-dimensional coupling-constant space given as a solution of a system of $2k$ equations for $2k$ couplings and one parameter r. We expect critical couplings to be such that for even k the coupling of the term with highest power ϕ^{4k} to be negative. The singular part of susceptibility will be described by a function h^2, where $h(t)$ satisfies a differential equation of order $2k$. We expect them to be the same string equations as in unitary matrix models which are related to the modified KdV hierarchy.

V. PERIOD-q *ANSATZ* AND MULTIBAND STRUCTURE

In this section we consider a q-component *Ansatz* for the coefficients R_n and discuss its relation to the multiband structure of the matrix model.

Let us assume that R_n has a period-q structure in the large-N limit so that $R_n\to A_\sigma(x)$, $x=n/N$, where $\sigma=n$

(mod$q$), $q \geq 3$. This corresponds to a q-component *Ansatz*. In the large-N limit, the free energy (3.1) becomes

$$\Gamma \rightarrow \text{const} - \frac{1}{q} \sum_{\sigma=1}^{q} \int_0^1 dx (1-x) \ln A_\sigma(x) . \tag{5.1}$$

We can again consider our Hilbert space as a direct sum of q subspaces $\mathcal{H}_\sigma$, $\mathcal{H} = \oplus_\sigma \mathcal{H}_\sigma$, where each $\mathcal{H}_\sigma$ is spanned by $\{|n\rangle, n = qp+\sigma, p = 0,1,2,\ldots\}$. Therefore, $\hat{G}$ can be written as a $q \times q$ matrix where each component $\hat{G}_{\sigma,\sigma'}$ maps $\mathcal{H}_{\sigma'}$ to $\mathcal{H}_\sigma$. In the large-N limit, under a q-component *Ansatz*, the generating function $(1/N)\sum_n \langle n|\hat{G}|n\rangle$ becomes

$$F^{(q)} = \frac{1}{q} \int_0^1 dx \sum_\sigma \int_0^{2\pi} \frac{d\theta}{2\pi} G_{\sigma,\sigma}(x,\theta) , \tag{5.2}$$

where $G_{\sigma,\sigma}(x,\theta)$ is a diagonal element of $[z - \phi(x,\theta)]^{-1}$. The $q \times q$ Hermitian matrix $\phi(x,\theta)$ has matrix elements

$$\phi_{\sigma,\sigma'}(x,\theta) = \sqrt{A_\sigma(x)}\,\delta_{\sigma,\sigma'+1} e^{i\theta} + \sqrt{A_{\sigma'}(x)}\,\delta_{\sigma,\sigma'-1} e^{-i\theta} , \tag{5.3}$$

where $\sigma = 1,2,\ldots,q$ (mod$q$).

It is convenient to use symmetric combinations $\eta(x) \equiv \sum_{\sigma=1}^q A_\sigma(x)$ and $\xi \equiv \prod_{\sigma=1}^q A_\sigma(x)$. For $q=3$, (5.2) can be greatly simplified, and one obtains

$$F^{(3)}(z) = \frac{1}{3} \int_0^1 dx \int_0^{2\pi} \frac{d\theta}{2\pi} \frac{3z^2-\eta}{z(z^2-\eta) - \sqrt{\xi}(e^{3i\theta}+e^{-3i\theta})} = \frac{1}{3} \int_0^1 dx \frac{3z^2-\eta(x)}{\{z^2[z^2-\eta(x)]^2 - 4\xi(x)\}^{1/2}} . \tag{5.4}$$

It can be checked for consistency that (5.4) reduces to (3.7) if all three A's are equal.

It is not difficult to simplify (5.2) for q up to 6. For completeness, we provide formulas for $q=4$ and 6:

$$F^{(4)}(z) = \frac{z}{4} \int_0^1 dx \frac{4z^2 - 2\eta(x)}{\{[z^4 - \eta(x) z^2 + \zeta_4(x)]^2 - 4\xi(x)\}^{1/2}} , \tag{5.5}$$

$$F^{(6)}(z) = \frac{z}{6} \int_0^1 dx \frac{6z^4 - 4\eta(x) z^2 + 2\zeta_6(x)}{\{[z^6 - \eta(x) z^4 + \zeta_6(x) z^2 - \epsilon_6(x)]^2 - 4\xi_6(x)\}^{1/2}} , \tag{5.6}$$

where $\zeta_4 \equiv A_1 A_3 + A_2 A_4$, $\zeta_6 \equiv \sum'_{\sigma,\sigma'} A_\sigma A_{\sigma'}$, and $\epsilon_6 \equiv A_1 A_3 A_5 + A_2 A_4 A_6$. ($\sum'_{\sigma,\sigma'}$ denotes that the sum runs over all nonadjacent pairs of A_σ's. For $q=6$, there are nine distinct pairings of this type.) It is also easy to check that both (5.5) and (5.6) reduce to $F^{(2)}(z)$ or $F^{(3)}(z)$ in appropriate limits where some A_σ's are equal.

It is *a priori* unclear for which potentials a particular q *Ansatz* would be appropriate in the large-N limit. It is plausible to assume that a large-q *Ansatz* would involve situations where a large number of local minima exist. For our current applications, we are primarily interested in situations where a three-band structure can occur. We have seen in Sec. III that, generically, when a potential has a pair of degenerate local minima, a two-component *Ansatz* becomes operative. The simplest generalization is one where a potential has three degenerate minima, e.g.,

$$U_6(\phi) \equiv \frac{\mu}{2}\phi^2 + \frac{g}{4}\phi^4 + \frac{\lambda}{6}\phi^6 = \frac{\lambda}{6}\phi^2(\phi^2-\phi_0^2)^2 .$$

The minima occur at $\phi = 0$, and $\phi = \pm\phi_0$, where $\phi_0^2 = -3g/4\lambda = -4\mu/g$. That is, for $\lambda > 0$, we restrict ourselves to the surface $g = -\sqrt{16\mu\lambda/3}$, $\mu > 0$, $g < 0$. In Fig. 2(a) the intersection of this surface with the I-III transition surface c is marked as β. Our numerical result in Fig. 7 suggests a period-3 *Ansatz* when U has three minima. We demonstrate below that, for this highly symmetric situation where the minima are degenerate, a period-3 *Ansatz* as formulated above indeed leads to a correct description of the three-band structure.

Under the period-3 *Ansatz*, (3.4) in the spherical limit leads to three coupled equations which, when expressed in terms of $\eta(x)$ and $\xi(x)$, become

$$x = A_\sigma[\mu + g\eta(x) + \lambda\eta(x)^2] + \lambda\xi(x) , \tag{5.7}$$

for $\sigma = 1,2,3$. Assuming that at least one pair of A_σ's are distinct, it follows that (5.7) leads to a pair of independent equations:

$$\lambda\eta^2 + g\eta + \mu = 0, \quad \xi = x/\lambda . \tag{5.8}$$

However, these two conditions are incompatible for x sufficiently large. (Since A_σ must be positive, as ξ increases with x without bound, η must also increase with x, which is not compatible with the first condition.) Therefore, we are again faced with a situation where there exists an $\bar{x}$, beyond which all three $A_\sigma(x)$ must become equal. Setting $\eta = 3r_0$ and $\xi = r_0^3$ in (5.8), one finds that

$$\bar{x} = \lambda r_0^3, \quad r_0 = \left| \frac{\mu}{3\lambda} \right|^{1/2} . \tag{5.9}$$

For $\bar{x} > 1$, with $g = -\sqrt{16\mu\lambda/3}$, (5.4) can be integrated easily and one obtains $F^{(3)}(z) = \frac{1}{2}U_6'(z) - i\pi\rho(z)$, where

$$\rho(z) = \frac{1}{2\pi}\lambda(z^2-r_0)[(z^2-r_1)(z^2-r_2)(r_3-z^2)]^{1/2} , \tag{5.10}$$

and the r's satisfy $0 < r_1 < r_0 < r_2 < r_3$, $r_1 r_2 r_3 = 4/\lambda$, $r_1 + r_2 r_3 = 6r_0$, and $r_1 r_2 + r_2 r_3 + r_3 r_1 = 9r_0^2$. The positive normalized spectral density (5.10) represents a three-band structure and solves the Schwinger-Dyson equation when the potential has three degenerate minima, as can be checked from (A1) and (A2).

For $\bar{x} < 1$, $F^{(3)}(z)$ can be shown to agree with $F^{(1)}(z)$ obtained by analytic continuation, thus describing a one-band structure. The transition between the three- and one-band phases occurs at $\bar{x} = 1$, where $r_0 = r_1 = r_2 \equiv r$.

This corresponds to the line

$$g=-\tfrac{4}{9}\mu^2,\quad \lambda=\tfrac{1}{27}\mu^3,\quad \mu>0\ , \tag{5.11}$$

which has been marked as the point β in Fig. 4(a).

Surprisingly, we find that the three-component *Ansatz* as formulated above is incompatible for U_6 away from the situation of three degenerate minima. Although (5.4) would produce a real analytic function $F(z)$ having the structure of a three-band phase, it turns out that in general $\mathrm{Re}F(z)\neq\frac{1}{2}U'(z)$ on the cuts. It is apparent that to produce an acceptable three-band solution everywhere, one needs to generalize the *Ansatz*. This will be discussed in another publication.

Finally, in this section we discuss a double-scaling limit around the point β and present the corresponding nonperturbative solution. We have learned from the planar limit analysis in Sec. II that the nature of the singularity at β corresponds to $k=1$. This and the previous discussion of the period-3 case suggest the scaling *Ansatz*

$$A^{(1)}_{n\pm j}=r+\epsilon^2 f(t\mp j\epsilon)+\epsilon a h(t\mp j\epsilon)$$
$$\text{for } n\pm j=3p+1\ ,$$
$$A^{(2)}_{n\pm j}=r+\epsilon^2 f(t\mp j\epsilon)+\epsilon b h(t\mp j\epsilon)$$
$$\text{for } n\pm j=3p+2\ ,$$
$$A^{(3)}_{n\pm j}=r+\epsilon^2 f(t\mp j\epsilon)-\epsilon(a+b)h(t\mp j\epsilon)$$
$$\text{for } n\pm j=3p\ ,$$

where t is defined by $x=1-\epsilon^2 t$ and $\epsilon=N^{-1/3}$. a and b are any nonzero real numbers. The results to be described do not depend upon the choice of a and b; in particular, $a=b$ is allowed. One can next write down three recursion relations for the $A^{(\sigma)}_n$, $\sigma=1,2,3$, and expand $f(t\mp j\epsilon)$ and $h(t\mp j\epsilon)$ in Taylor series as usual. Of these three equations, only two are independent, which we choose to be the sum of the three and the difference of the first and the third. Keeping terms up to the order ϵ, one finds that the coupling constants satisfy

$$10\lambda r^3+3gr^2+\mu r=1\ ,$$
$$9\lambda r^2+3gr+\mu=0\ ,$$
$$4\lambda r+g=0\ .$$

These equations specify a line in the coupling space which can be parametrized in terms of r by

$$\mu=\frac{3}{r},\quad g=-\frac{4}{r^2},\quad \lambda=\frac{1}{r^3}\ .$$

This is precisely the equation of the line β [Eq. (5.11)] that lies in the I-III phase boundary c; this shows that β is the only line at which the above double-scaling *Ansatz* is consistent. This agrees with our direct analysis using (5.4).

Expanding to order ϵ^3, we obtain two equations for the two functions f and h which have the same structure at the critical couplings as those found in Sec. IV. Eliminating $f(t)$, we obtain the $k=1$ Painlevé II equation for $h(t)$, [Eq. (4.4)]. Just as for the phase boundary between the one- and two-band phases, the singular part of the susceptibility is proportional to h^2. Again, we note that the $k=1$ Painlevé II solution is obtained at that point in coupling-constant space where a double zero of $\Delta(z)$ gets sandwiched between two coalescing bands (i.e., four zeros of Δ coalesce; see diagram for c in Table II), as in the case of the phase boundary a.

VI. CONCLUDING REMARKS

We return to the questions raised in the Introduction about the $k=2$ pure gravity solution. This solution is obtained as one approaches line b (Table II, Fig. 4) from the one-band phase. Note that line b lies partly in the existence domain of a two-band phase and wholly in the existence domain of the three-band phase. Thus three-band solutions necessarily coexist with the $k=2$ one-band solution (the latter will be referred to as the "pure gravity solution"), a fact that was also noted in Refs. 16 and 17. Since the three-band phase does not have a unique solution, there actually coexist at b a one-parameter family of three-band solutions, which, as discussed in Sec. II, can be labeled by the difference of the chemical potentials in the central band and sidebands, or by the location $\sqrt{r_0}$ of the double zero of $\Delta(z)$ [see (A1) and (2.5)].

Of these, consider the specific three-band solution (which we denote III_0) for which $r_0=r_1$ (i.e., the single zero of ρ is always coincident with the edge of the central band). This particular phase reaches its own phase boundary at the line b, where its sidebands vanish. (The phase boundaries of III_0 are b, c, and e.) We therefore expect this three-band solution III_0 to possess a double-scaling limit at b and hence provide a nonperturbative solution that coexists with pure gravity at b. Using the method described in Sec. II, we have found that the critical exponent for III_0 approaching b is given by $k=1$. This solution has the same free energy as the one-band solution at b, which can be seen by inspection of the diagram for b in Table II. However, this solution is not the dominant three-band solution close to b. The reason we expect this is that since $r_0=r_1$ for this solution, it follows by the argument indicated in Sec. II that the chemical potential for the central band and sidebands for this solution are very different, and hence this is unlikely to minimize the free energy. The dominant solution at b is likely to be a three-band solution with all bands of finite length. Such a solution will not exhibit double scaling at b.

For the one-band phase one intuitively expects that precisely at the boundary b the net energy barrier for an eigenvalue to tunnel out of the central band is zero. On the other hand, at a finite distance from b this barrier is $O(N)$. The situation has been analyzed in Ref. 17 where it has been shown that in the double-scaling limit of the one-band phase, the barrier for a single eigenvalue to tunnel through is of order 1. This means that all along the path of double scaling the pure gravity solution can tunnel into III_0. In view of this fact and the above observation that III_0 is likely to exhibit a nonperturbative solution at b, possibly of a new type, it is of interest to identify this solution and interpret what the coexistence means

for the nonperturbative string theory. Another interesting solution to be analyzed is the $k=1$ solution from the three-band phase at γ where the one-band phase gives the $k=3$ multicritical solution corresponding to the Lee-Yang model.[32]

A beginning in this direction has been made in this paper. In Sec. V we have exhibited one nonperturbative three-band solution at a specific point on the boundary c. However, our treatment does not cover the phase III_0 at b. Among other things, one needs to understand how the one-parameter freedom in choosing a three-band solution reflects itself in the *Ansatz* for the R_n.

We note here that all the $k=2$ solutions found in Hermitian one-matrix models so far arise either when the potential is unbounded from below [e.g., line b approached from the one-band phase in U_4 and line given by (4.5) approached from the two-band phase in U_8], or when the solution that gives rise to $k=2$ behavior is subdominant (as for the line b approached from the one-band phase in U_6). This is not the case for unitary one-matrix models[30] where a dominant $k=2$ solution seems to be possible in a well-defined model due to the periodicity of the potential. The implications of the present analysis of the phase structure for unitary models will be discussed elsewhere. The questions raised in this paper are also relevant for multimatrix models and the $d=1$ model. It is of interest to determine what new features in the phase structure arise when these models are regulated by a well-defined potential.[33]

In other approaches to 2D gravity, at this stage there does not seem to be any evidence of phases related to multiband phases of the matrix model. However, it would be worthwhile to explore, for example, whether there is a phase of topological gravity[34] that is related to the Painlevé II equation which seems to appear in multiband phases of the Hermitian matrix model and in unitary matrix models.

To summarize, we have discussed the multiband phase structure of Hermitian one-matrix models from two distinct viewpoints: the large-N Schwinger-Dyson equation and the orthogonal polynomial method. We have given a systematic way of comparing the two approaches and demonstrated in examples how periodicity in the recursion coefficients gives rise to multiband structure. Further, we have identified the double-scaling limit for two- and three-band phases at specific boundaries and obtained nonperturbative solutions which were not previously known to exist for the multiband phases of the Hermitian matrix model.

Note added. After the completion of this work, we became aware of Ref. 35, which also discusses the two-band phase at the tree level from the orthogonal polynomial method, using a technique that is different from ours.

ACKNOWLEDGMENTS

We would like to thank A. Jevicki and G. Mandal for discussions. N.D. and S.J. would like to thank the Aspen Center for Physics for its hospitality, where part of this work was done. This work was supported in part by the Department of Energy under Contract No. DE-AC02-76ERO3130.A021-Task A.

APPENDIX A: DETERMINATION OF PHASE BOUNDARIES

We present an example of the determination of phase boundaries by considering the case of a U_6 potential having a three-band phase. Using the schematic representation [Fig. 4(c)], one finds that

$$\Delta(z)=\lambda^2(z^2-r_0)^2(z^2-r_1)(z^2-r_2)(z^2-r_3)\ , \tag{A1}$$

where r_i's, $0<r_1\le r_0\le r_2\le r_3$, describe the locations of the zeros of Δ. As is apparent from (2.5), in the above configuration the central band consists of $z\in(-\sqrt{r_1},\sqrt{r_1})$, and the two sidebands $(\pm\sqrt{r_2},\pm\sqrt{r_3})$. By comparing the coefficients of z^4, z^6, and z^8 of this expression with that from the right-hand side of (2.4), we obtain three equations:

$$\begin{aligned}
&-\lambda^2[r_0^2(r_1+r_2+r_3)+2r_0(r_1r_2+r_2r_3+r_3r_1)\\
&\qquad +r_1r_2r_3]=2\mu g-4\lambda\ ,\\
&\lambda^2[2r_0(r_1+r_2+r_3)+r_0^2\\
&\qquad +(r_1r_2+r_2r_3+r_3r_1)]=g^2+2\mu\lambda\ ,\\
&\qquad -\lambda^2(2r_0+r_1+r_2+r_3)=2g\lambda\ .
\end{aligned} \tag{A2}$$

Every solution of (A2) for the r's gives a solution of the Schwinger-Dyson equation or, equivalently, a solution for ρ satisfying (2.1). This means that there is a one-parameter family of three-band solutions, which we may label by the value of r_0. We also note that (2.3) and (A1) allow one to determine w_2, w_4, etc., in terms of the r's and the couplings, e.g.,

$$w_2=\frac{1}{\lambda}\left[\frac{\mu^2}{4}-g\right]-\frac{\lambda}{4}[r_0^2(r_1r_2+r_2r_3+r_3r_1)+2r_0r_1r_2r_3]\ . \tag{A3}$$

When one reaches a phase boundary of the three-band phase, the zeros of Δ collide, reducing the number of unknowns from four to two (see Table II). Equation (A2) then allows a complete solution as well as provides a constraint among the couplings which is the equation of the surface constituting the phase boundary. For example, at c we have $r_0=r_1=r_2$. Equation (A2) then gives

$$\begin{aligned}
&r_0=\frac{1}{5\lambda}\left[-2g-\frac{\omega}{4}\right],\quad r_3=\frac{1}{5\lambda}(-2g+\omega)\ ,\\
&\omega\equiv[8(3g^2-10\mu\lambda)]^{1/2}\ ,
\end{aligned} \tag{A4}$$

and it provides the equation shown in Table II. For this case,

$$\rho(z)=\frac{1}{2\pi}\lambda(z^2-r_0)^2(r_3-z^2)^{1/2}\ \text{ for } 0\le z^2<r_3\ , \tag{A5}$$

and $\rho=0$ otherwise. Equations for other phase boundaries are obtained similarly.

At this point we also write down for convenience of referring in the text the expressions for $\rho(z)$ for the one- and two-band phases in U_4 when $\mu<0$ and $g>0$,[31] ob-

tained by solving the Schwinger-Dyson equation. For the one-band phase depicted by the first diagram in Fig. 3(a), we have

$$\rho(z)=\frac{1}{2\pi}g(z^2-r_0)(r_1-z^2)^{1/2} \quad \text{for } 0\le z^2\le r_1 , \tag{A6}$$

where

$$r_0=\frac{2}{3g}\left[-\mu-\frac{v}{2}\right]<0, \quad r_1=\frac{2}{3g}(-\mu+v)>0 ,$$
$$v\equiv(\mu^2+12g)^{1/2} . \tag{A7}$$

[$\rho(z)$ is zero outside the region displayed.] For the two-band phase depicted in Fig. 3(b),

$$\rho(z)=\frac{1}{2\pi}gz[(z^2-r_1)(r_2-z^2)]^{1/2} \quad \text{for } r_1\le z^2\le r_2 , \tag{A8}$$

where

$$r_1=\frac{1}{g}(-\mu-2\sqrt{g}), \quad r_2=\frac{1}{g}(-\mu+2\sqrt{g}) . \tag{A9}$$

APPENDIX B: DETERMINATION OF CRITICAL EXPONENTS

Consider approaching the phase boundary c from the three-band phase along the surface $g^2=\frac{16}{3}\mu\lambda$, which intersects c at the line β [see Fig. 2(a)]. For purposes of this calculation, we choose a path of approach that lies in the plane $\lambda=\frac{1}{8}$; hence the coordinates of β are $\mu_c=\frac{3}{2}$, $g_c=-1$, and $\lambda_c=\frac{1}{8}$. To be in region III near this point, one can parametrize $g=g_c-t$, $t\ge 0$. Then, along the curve of approach, $\mu=\frac{3}{2}(g_c-t)^2$.

To determine k we need w_2 as a function of μ, g, and λ in the three-band phase. As noted in Appendix A, this requires making a choice of r_0. From (A4) one finds that r_0 must take on the value $-g_c/4\lambda_c$ at the critical point. We choose the particular solution with $r_0=-g/4\lambda$ all along the curve. This special choice is motivated by the desire to compare with results from the method of orthogonal polynomials in Sec. V, but is not necessary. We expect other choices to give the same result for k. With this choice, r_1, r_2, r_3, and w_2 are determined from (A2) and (A3) as functions of t. This calculation was done by using MACSYMA. For small t it was found that

$$w_2=-\tfrac{5095}{2}-10214t$$
$$-(344\,064\sqrt{3}-49\,562\,341)t^2+O(t^3) . \tag{B1}$$

No singular terms in t were obtained. This means that when c is approached at β from the three-band phase, we have $k=1$. The same method gave $w_2\sim t^{4/3}$, corresponding to $k=3$ when the curve γ was approached from the one-band phase.

*On leave of absence from Rudjer Bošković Institute, Zagreb, Croatia, Yugoslavia.
†Also at Department of Physics, Mount Holyoke College, S. Hadley, MA 01075.
‡Present address: Department of Physics, Harvard University, Cambridge, MA 02138.

[1]V. A. Kazakov, Phys. Lett. **150B**, 282 (1985); F. David, Nucl. Phys. **B257**, 45 (1985); **B257**, 543 (1985); J. Ambjørn, B. Durhuus, and J. Fröhlich, *ibid.* **B257**, 433 (1985); V. A. Kazakov, I. K. Kostov, and A. A. Migdal, Phys. Lett. **157B**, 295 (1985).
[2]V. A. Kazakov, Mod. Phys. Lett. A **4**, 2125 (1989).
[3]G. 't Hooft, Nucl. Phys. **B72**, 461 (1974).
[4]E. Brézin, C. Itzykson, G. Parisi, and J. B. Zuber, Commun. Math. Phys. **59**, 35 (1978).
[5]D. J. Gross and E. Witten, Phys. Rev. D **21**, 446 (1980); S. R. Wadia, Chicago University Report No. EFI-79/44, 1979 (unpublished).
[6]R. Brower, P. Rossi, and C.-I Tan, Phys. Rev. D **23**, 942 (1981); **23**, 953 (1981).
[7]E. Brézin and V. A. Kazakov, Phys. Lett. B **236**, 144 (1990); M. R. Douglas and S. H. Shenker, Nucl. Phys. **B335**, 635 (1990); D. J. Gross and A. A. Migdal, Phys. Rev. Lett. **64**, 127 (1990).
[8]E. Brézin, M. R. Douglas, V. A. Kazakov, and S. H. Shenker, Phys. Lett. B **237**, 43 (1990); D. J. Gross and A. A. Migdal, Phys. Rev. Lett. **64**, 771 (1990); Č. Crnković, P. Ginsparg, and G. Moore, Phys. Lett. B **237**, 196 (1990).
[9]M. R. Douglas, Phys. Lett. B **238**, 176 (1990).
[10]E. Brézin, V. A. Kazakov, and Al. B. Zamolodchikov, Nucl. Phys. **B338**, 673 (1990); D. J. Gross and N. Miljković, Phys. Lett. B **238**, 217 (1990); G. Parisi, *ibid.* **238**, 209 (1990); P. Ginsparg and J. Zinn-Justin, *ibid.* **240**, 333 (1990).
[11]A. M. Polyakov, Phys. Lett. **103B**, 207 (1981); V. G. Knizhnik, A. M. Polyakov, and A. B. Zamolodchikov, Mod. Phys. Lett. A **3**, 819 (1988).
[12]F. David, Mod. Phys. Lett. A **3**, 1651 (1988); J. Distler and H. Kawai, Nucl. Phys. **B321**, 509 (1989).
[13]S. R. Das, S. Naik, and S. R. Wadia, Mod. Phys. Lett. A **4**, 1033 (1989); A. Dhar, T. Jayaraman, K. S. Narain, and S. R. Wadia, *ibid.* **5**, 863 (1990); S. R. Das, A. Dhar, and S. R. Wadia, *ibid.* **5**, 799 (1990); T. Banks and J. Lykken, Nucl. Phys. **B331**, 173 (1990); A. A. Tseytlin, Int. J. Mod. Phys. A **5**, 1833 (1990).
[14]I. K. Kostov and A. Krzywicki, Phys. Lett. B **187**, 149 (1987); I. K. Kostov and M. L. Mehta, *ibid.* **189**, 118 (1987).
[15]G. M. Cicuta, L. Molinari, and E. Montaldi, J. Phys. A **23**, L421 (1990).
[16]J. Jurkiewicz, Phys. Lett. B **245**, 178 (1990).
[17]G. Bhanot, G. Mandal, and O. Narayan, IAS Report No. IASSNS-HEP-90/52, 1990 (unpublished).
[18]E. Brézin, E. Marinari, and G. Parisi, Phys. Lett. B **242**, 35 (1990).
[19]M. R. Douglas, N. Seiberg, and S. H. Shenker, Phys. Lett. B **244**, 381 (1990).
[20]F. David, Mod. Phys. Lett. A **5**, 1019 (1990); Saclay report, 1990 (unpublished).
[21]T.-L. Chen, C.-I. Tan, and Z.-T. Zheng, Phys. Lett. **123B**, 423 (1983); J. Jurkiewicz and K. Zalewski, Nucl. Phys. **B220**, 167

(1983).
[22]G. Mandal, Mod. Phys. Lett. A **5**, 1147 (1990).
[23]D. Friedan, Commun. Math. Phys. **78**, 353 (1981).
[24]S. R. Wadia, Phys. Rev. D **24**, 970 (1981).
[25]M. L. Mehta, *Random Matrices* (Academic, New York, 1967).
[26]D. Bessis, Commun. Math. Phys. **69**, 147 (1979).
[27]D. Bessis, C. Itzykson, and J. B. Zuber, Adv. Appl. Math. **1**, 109 (1980).
[28]L. Molinari, J. Phys. A **21**, 1 (1988).
[29]D. J. Gross and A. A. Migdal, Nucl. Phys. **B340**, 333 (1990); T. Banks, M. R. Douglas, N. Seiberg, and S. H. Shenker, Phys. Lett. B **238**, 279 (1990).
[30]V. Periwal and D. Shevitz, Phys. Rev. Lett. **64**, 1326 (1990); K. Demeterfi and C.-I Tan, Mod. Phys. Lett. A **5**, 1563 (1990).
[31]Y. Shimamune, Phys. Lett. **108B**, 407 (1982).
[32]M. Staudacher, Nucl. Phys. **B336**, 349 (1990).
[33]We have learned that for $d=1$ numerical results relevant to this question have been recently obtained by the authors of Ref. 17 (private communication).
[34]E. Witten, Nucl. Phys. **B340**, 281 (1990).
[35]L. Molinari and E. Montaldi, INFN Milano University report (unpublished).